



Condensation and immersion freezing Ice Nucleating Particle measurements at Ny-Ålesund (Svalbard) during 2018: evidence of multiple source contribution

Matteo Rinaldi¹, Naruki Hiranuma², Gianni Santachiara¹, Mauro Mazzola³, Karam Mansour^{1,4,5}, Marco Paglione¹, Cheyanne A. Rodriguez², Rita Traversi⁶, Silvia Becagli⁶, David M. Cappelletti⁷, Franco Belosi¹

¹Institute of Atmospheric Sciences and Climate (ISAC), National Research Council (CNR), 40129 Bologna, Italy

²Department of Life, Earth and Environmental Sciences, West Texas A&M University, Canyon, TX, USA

³Institute of Polar Sciences (ISP), National Research Council (CNR), 40129 Bologna, Italy

⁴Department of Physics and Astronomy, University of Bologna, 40127 Bologna, Italy

⁵Department of Oceanography, Faculty of Science, University of Alexandria, 21511 Alexandria, Egypt

⁶Department of Chemistry “Ugo Schiff”, University of Florence, 50019 Florence, Italy

⁷Dipartimento di Chimica, Biologia e Biotecnologie, Università degli Studi di Perugia, 06123 Perugia, Italy

Correspondence to: Matteo Rinaldi (m.rinaldi@isac.cnr.it)

Abstract. The current inadequate understanding of ice nucleating particle (INP) sources in the Arctic region affects the uncertainty in global radiative budgets and in regional climate predictions. In this study, we present atmospheric INP concentrations by offline analyses on samples collected at ground level in Ny-Ålesund (Svalbard), in spring and summer 2018. The ice nucleation properties of the samples were characterized by means of two offline instruments: the Dynamic Filter Processing Chamber (DFPC), detecting condensation freezing INPs, and the West Texas Cryogenic Refrigerator Applied to Freezing Test system (WT-CRAFT), measuring INPs by immersion freezing.

Both measurements agreed within an order of magnitude although with some notable offset. INP concentration measured by DFPC ranged 33-185 (median 88), 5-107 (50) and 3-66 (20) m⁻³, for T = -22, -18 and -15°C, respectively, while at the same activation temperatures WT-CRAFT measured 3-199 (26), 1-34 (6) and 1-4 (2) m⁻³, with an offset apparently dependent on the INP activation temperature. This observation may indicate a different sensitivity of Arctic INPs to different ice nucleation modes, even though a contribution from measurement and/or sampling uncertainties cannot be ruled out.

An increase in the coarse INP fraction was observed from spring to summer, particularly at the warmest temperature (up to ~70% at -15°C). This suggests a non-negligible contribution from local sources of biogenic aerosol particles. This conclusion is also supported by the INP temperature spectra, showing ice-forming activity at temperatures higher than -15°C. Contrary to recent works (e.g., INP measurements from Ny-Ålesund in 2012), our results do not show a sharp spring-to-summer increase of the INP concentration, with distinct behaviors for particles active in different temperature ranges. This likely indicates that the inter-annual variability of conditions affecting the INP emission by local sources may be wider than previously considered and suggests a complex interplay between INP sources. This demonstrates the necessity of further data coverage.



Analysis of INP concentrations, active site density, low-travelling back-trajectories (< 500m) and ground conditions during the air mass passage suggest that the summertime INP population may be contributed both by terrestrial and marine sources.

35 Air masses in contact with snow-free land had higher INP concentrations, likely reflecting the higher nucleation ability of terrestrial particles. Outside the major terrestrial inputs, the INP population was likely regulated by marine INPs emitted from the sea surface. Evidence of the relation between background INP concentration and the patterns of marine biological activity have been provided by investigating its spatio-temporal correlation with satellite retrieved Chlorophyll-a fields and by the Concentration Weighted Trajectory (CWT) model. The results suggest that sources of INPs may be located both in the

40 seawaters surrounding the Svalbard archipelago and/or as far as Greenland and Iceland.

1 Introduction

The Arctic is a climate-change sensitive region and is experiencing a higher temperature increase if compared to mid latitudes (the so called “Arctic amplification”). Many different atmospheric processes and feedback mechanisms contribute to the Arctic amplification (Goosse et al., 2018;Pithan and Mauritsen, 2014), whose key parameters are cloud fraction, cloud water content

45 and phase, aerosol particle size and temperature (Curry et al., 1996;Garrett et al., 2009;Kay et al., 2011). The majority of these feedbacks are presently not understood in detail. Aerosols, and in particular their capacity of affecting cloud thickness, lifetime, and albedo, are the least constrained atmospheric components affecting radiative budgets (Boucher and Quaas, 2013;Lee et al., 2016;Stocker et al., 2013).

Clouds in the Arctic are often mixed-phase (comprising both ice and supercooled liquid water) and structured in persistent stratiform layers (Shupe et al., 2006;Choi et al., 2010;Costa et al., 2017;Shupe et al., 2011). Feedbacks between numerous

50 local processes, including the formation and growth of ice and cloud droplets, radiative cooling, turbulence, entrainment and surface fluxes of heat and moisture, interact to create a resilient mixed-phase cloud system (Morrison et al., 2012 and references therein). Thus, the presence of sufficient numbers of particles that can trigger heterogeneous ice nucleation (ice nucleating particles, INPs) in the Arctic atmosphere can potentially have large impacts on cloud radiative properties and precipitations

55 (Prenni et al., 2007;Solomon et al., 2018;Lohmann, 2002). For these reasons, the current inadequate understanding of INP sources and transport dynamics in the Arctic region impacts heavily on the uncertainties in Northern latitudes surface radiative budgets.

In general, INPs can be of abiotic (e.g., mineral dust, volcanic ashes and soil dust) or biotic (e.g., bacteria, fungi, microalgae and pollen) origin (Hoose and Moehler, 2012;Murray et al., 2012). Sea water has recently been showed to be a source of ice

60 active organic matter (Knopf et al., 2011;Wang et al., 2015;Wilson et al., 2015), transferable to the atmosphere within sea spray particles (DeMott et al., 2016;McCluskey et al., 2017;McCluskey et al., 2018b;Ickes et al., 2020). Most ice nucleation processes below -15°C are driven by the presence of mineral particles, which are considered inactive at higher temperatures. (Hoose and Moehler, 2012;Murray et al., 2012;Kanji et al., 2017;DeMott et al., 2010). In contrast, biogenic INPs have ice nucleation properties that support formation of clouds, rain, and snow at temperatures $\geq -15^{\circ}\text{C}$ (Murray et al., 2012;Hoose and



65 Moehler, 2012;Frohlich-Nowoisky et al., 2015;Tesson and Santl-Temkiv, 2018;O'Sullivan et al., 2014;O'Sullivan et al.,
2015;Conen et al., 2011).

Not many measurements of INP exist in the Arctic at present and the available data cover mostly short periods of time. The
first ground level INP data reported in literature for the Arctic atmosphere are those by Borys (1983;1989). Measurements
were performed with T between -28 and -16°C and the observed INP concentration (n_{INP}) ranged between less than 10 to ca.
70 500 m⁻³. It was hypothesized that pollution from lower latitudes did not contribute significantly INPs to the Arctic atmosphere,
as low n_{INP} values characterized the winter period, when Arctic haze, originating from anthropogenic pollution, was present.
This was recently confirmed by Hartmann et al. (2019) through the analysis of ice core records. Later on, Bigg (1996) and
Bigg and Leck (2001) measured INP active at -15°C in a static chamber and at humidity just above 100%, during icebreak
cruises to the central Arctic ocean (August –October 1991 and July –September 1996). The Ocean was identified as the main
75 source of INPs.

More recent measurements were mostly performed in the immersion freezing mode. Conen et al. (2016), at a coastal mountain
observatory in Northern Norway, measured in summer a tripling INP ($T = -15^\circ\text{C}$) concentration in oceanic air after about one
day of passage over land. Both marine and terrestrial INP sources were evidenced by Creamean et al. (2018) in the Northern
Alaskan Arctic, during spring. Irish et al. (2019) measured INP concentrations, in the Canadian Arctic marine boundary layer,
80 during summer 2014, on board the CCGS Amudsen. INP concentrations were positively correlated with the total residence
time over land and negatively correlated with the total residence time over sea ice and open water, suggesting higher
contribution of mineral dust particles than sea-spray related sources. Similar conclusions were reached by Si et al. (2018) from
measurements performed in the Canadian Arctic. Mason et al. (2016) evidenced that a large fraction of the observed INPs
belonged to the coarse size range, through spring and summer time measurements at Alert station. Consistently, a size
85 dependent ice nucleation efficiency, with larger particles being more ice active, was reported by Creamen et al. (2018) and Si
et al. (2018).

Recently, a marked n_{INP} seasonal trend in the Arctic environment was reported (Wex et al., 2019;Tobo et al., 2019;Santl-
Temkiv et al., 2019), evidencing order of magnitude wise increase in the atmospheric loadings from spring to summertime.
This increase was interpreted as the effect of local INP sources active when land and sea are free from snow and ice. Such a
90 seasonality did not emerge clearly from the previous measurements enlisted above, mainly because of the reduced time
coverage of the observations. Conversely, Schrod et al. (2017) reported a flat seasonal trend for measurements performed
between May 2015 and May 2016 at Mt. Zeppelin (Svalbard), suggesting high inter-annual variability in the INP seasonal
pattern.

In the present study, we contribute to fill the present gap of INP observations in the Arctic environment, investigating the INP
95 concentration and potential sources at Ny-Ålesund (Svalbard), through spring and summer time measurements by two INP
quantification techniques.



2 Methods

2.1 Sampling

The aerosol sampling was performed at the Gruvebadet observatory, located in proximity of the village of Ny-Ålesund (78°55' N, 11°56' E) on the Spitsbergen Island, Svalbard. The observatory is about 70 m above sea level, located about 1 Km south-west of the village. This position guarantees that the aerosol samples are not affected by local sources of pollution, being the main wind flow from southeast (Udisti et al., 2016). Aerosol sampling for INP quantification analyses occurred independently for the two methods. Nevertheless, the inlets were all located at the same altitude, about 1 m above the building roof.

For the Dynamic Filter Processing Chamber (DFPC; see Par 2.2.1) aerosol samples were collected on nitrocellulose membrane filters (Millipore HABG04700, nominal porosity 0.45 μm) by deploying two parallel sampling systems, one equipped with a PM_1 inlet and the other with a PM_{10} one (cut-point-Standard EN 12341, TCR Tecora). The operative flow was 38.3 lpm in each sampling line and was generated by two independent pumps (Bravo H Plus, TCR Tecora). Sampling for DFPC occurred on an intensive campaign basis. The spring campaign occurred between 17 April and 2 May 2018, while the summer campaign covered the period between 11 and 27 July 2018. One couple of samples ($\text{PM}_1/\text{PM}_{10}$) was collected per day, with a sampling duration between 3 and 4 hours, to avoid filter overloading. The sampling generally started in the morning, during the spring campaign, while it started typically in the afternoon during the summer campaign. Samples were stored at room temperature until analysis.

For the West Texas Cryogenic Refrigerator Applied to Freezing Test system (WT-CRAFT; see Sect. 2.2.2) analysis, a total of 28 aerosol filter samples were collected using 47 mm membrane filters (0.2 μm pore size). Briefly, particle-laden air was drawn through a central TSP inlet with a constant inlet flow of 150 lpm. From the inlet, an 8 mm OD stainless steel tube was directly connected to the filter sampler. Below the filter sampler, the filtered-air was constantly pumped through a diaphragm pump. It is noteworthy that a critical orifice was installed upstream of the pump to ensure a constant volume flow rate and control the mass flow rate through the sampling line. A typical sampling interval was approximately of 4 days with only one exception (i.e., 8 days for the sample collected starting on 26 May 2018).

2.2 Ice Nucleation Measurements

2.2.1 DFPC

INP concentrations were quantified in the lab, after completion of the campaigns, by the membrane filter technique (Bigg et al., 1963; Vali, 1975) following the procedure presented in Santachiara et al. (2010) and described in Rinaldi et al. (2017). A replica of the Langer dynamic filter processing chamber housed in a refrigerator was used to determine the concentration of aerosol particles active as INP at different temperatures. Measurements were performed at activation temperatures (T) of -15°C, -18°C and -22°C and at water saturation ratio (S_w) = 1.02. Uncertainties for temperature and S_w are about 0.1 °C and 0.02, respectively. Consequently, the estimated, INP measurement uncertainty of the DFPC is $\pm 30\%$ (DeMott et al., 2018).



Examples of inter-comparisons between the DFPC and other INP quantification techniques can be found in DeMott et al. (2018), McCluskey et al. (2018b) and Hiranuma et al. (2019).

130 2.2.2 WT-CRAFT

To complement the DFPC results, we also used an offline droplet-freezing assay instrument, the WT-CRAFT, to measure temperature-resolved INP concentrations at $T > -25$ °C, with a detection capability of >1 INP per m^{-3} of air. While WT-CRAFT is originally a replica of NIPR-CRAFT (Tobo, 2016), the two CRAFT systems possess different sensitivities to artifact and detectable T ranges as described in Hiranuma et al. (2019). As shown in Hiranuma et al. (2019, i.e., Table S2), the uncertainties of temperature as well as ice nucleation efficiency in WT-CRAFT are ± 0.5 °C and $\pm 23.5\%$, respectively. Other detailed descriptions of WT-CRAFT are provided in Hiranuma et al. (2019), Cory et al. (2019), and Whiteside et al. (2019). Therefore, we only give a brief method description of WT-CRAFT specific to this study. For each experiment, 70 solution droplets (3 μL each) placed on a hydrophobic Vaseline layer were analyzed. With a cooling rate of 1 °C min^{-1} , we manually counted cumulative number of frozen droplets based on the color contrast shift in the off-the-shelf video recording camera. Afterwards, INP concentration of super-microliter-sized droplets containing particles from the samples were estimated as a function of T for every 0.5 °C. Prior to each WT-CRAFT experiment, we suspended particles on an individual filter sample in a known volume of ultrapure water (HPLC grade), in which the first frozen droplet corresponded to 1 INP per m^{-3} . More specifically, our suspension-generating protocol followed (1) cutting the filter in two and soaking one filter half in ultrapure water in a sterilized falcon tube, (2) applying a mechanical vibration to the suspension tube to scrub particles on the filter in suspension, (3) applying an idle time of 5 min to have the quasi-steady state suspension, and (4) preparation of droplets out of the suspension. If necessary, the suspension sample was diluted until we observe their freezing spectrum collapsed onto the water background curve. It is noteworthy that our diluted spectra and original freezing spectrum reasonably agreed in their overlapped T region (within a factor of three at the most) without any notable artifacts at T above -25 °C. Due to the absence of failure, we simply stitched all spectra in the way that the diluted spectrum followed up and took over the cold temperature data points immediately after the last data point of less diluted spectrum.

2.2.3 Ice Nucleation Parameterizations

The atmospheric concentration of ice nucleating particles (n_{INP}), expressed hereafter in units of m^{-3} , was calculated, for each technique, by dividing the number of INP quantified for each sample by the total volume of air passed through the corresponding filter. The ice nucleating active site density (n_s) was derived as in Niemand et al. (2012), by normalizing the INP number concentration for the total aerosol surface in the range between 10 nm and 10 μm (see next paragraph for details), calculated under the assumption of spherical particles.



2.3 Complementary Analyses

2.3.1 Particle size distribution measurements

The aerosol particle number size distribution is continuously monitored at Gruebadet since 2010 using a Scanning Mobility Particle Sizer (SMPS) model TSI 3034 for the diameter range between 10 and 500 nm (54 channels) and an Aerodynamic Particle Sizer (APS) model TSI 3321 for the diameters above 500 nm (same number of channels as the SMPS). Both instruments are connected to a common multiple inlet with laminar flow (the same where the sampling for the WT-CRAFT analysis was performed) and record data averaged over 10 minutes (Giardi et al., 2016; Lupi et al., 2016). The aerodynamic diameters reported by the APS were corrected to real physical diameters using a particle mass density equal to 1.95 g cm^{-3} and the number concentration in the resulting overlapping range was taken equal to that from the SMPS.

2.3.2 Meteorology

Meteorological parameters (air temperature, T; pressure, P; relative humidity, RH; wind speed, WS) were taken from those continuously provided by the Amundsen-Nobile Climate Change Tower, positioned less than 1 Km N-E of Gruebadet (Mazzola et al., 2016), while precipitation data (type and amount) from the eKlima database, provided by the Norwegian Meteorological Institute (<https://seklima.met.no/observations/>).

2.3.3 Offline Chemical Analysis

The chemical analysis of major and trace ion species, used in this work as aerosol source tracers, was accomplished on filters collected at GVB. The filters were handled in conditions of minimal contamination (working under a class 100 laminar flow hood) during all the phases of the analytical procedure. The measurements were carried out by a triple Dionex ThermoFisher Ion Chromatography system equipped with electrochemical-suppressed conductivity detectors. In particular, a Dionex AS4A-4 mm analytical column with a $1.8 \text{ mM Na}_2\text{CO}_3/1.7 \text{ mM NaHCO}_3$ eluent, was used for the determination of most of inorganic anions (Cl^- , NO_3^- , SO_4^{2-} , $\text{C}_2\text{O}_4^{2-}$) while a Dionex AS11 separation column with a gradient elution ($0.075\text{--}2.5 \text{ mM Na}_2\text{B}_4\text{O}_7$ eluent) was used for the measurement of F^- and some organic anions (acetate, glycolate, formate and methanesulfonate). Cationic species (Na^+ , NH_4^+ , K^+ , Mg_2^+ , Ca_2^+) have been determined by a Dionex CS12A-4 mm analytical column with $20 \text{ mM H}_2\text{SO}_4$ as eluent. Further analytical details can be found in Udisti et al. (2016) and Becagli et al. (2011).

2.3.4 Back trajectories and satellite ground type maps

The ground types over which air masses travelled in the 5 days before arrival at GVB station were identified, for both DFPC and WT-CRAFT samples, following Wex et al. (2019). The considered ground types were seawater, sea-ice, land, and snow (over land). For this analysis, five-day back-trajectory air masses (HYSPLIT4 with GDAS data: <https://ready.arl.noaa.gov/>) from the National Oceanic and Atmospheric Administration (NOAA) HYSPLIT model (Rolph et al., 2017; Stein et al., 2015) arriving at an altitude of 100 m (amsl) over GVB station were calculated. For DFPC samples, the back-trajectories arrival time



was considered simultaneous to INP samples, while for WT-CRAFT, the trajectories were calculated 4 times (00, 06, 12 and 18 UTC) a day covering the INP sampling period from April to August.

Ground condition maps were obtained from the National Ice Center's Interactive Multisensor Snow and Ice Mapping System (IMS) (Helfrich et al., 2007; National Ice-Center, 2008), National Snow & Ice Data center (NISDC; <https://nsidc.org/>). IMS maps are a composite product produced by NOAA/NESDIS (National Environmental Satellite Data and Information Service) combining information on both sea ice and snow cover. Information from 15 different sources of input is included in the production of these maps (Helfrich et al., 2007). We used the daily Northern Hemisphere maps with a resolution of 4 km. For each back-trajectory time step, we applied nearest-neighbour interpolation in space and time to find the corresponding satellite coordinate along the back trajectory. Consequently, the ground type conditions during air mass passage were determined. It is worth highlighting that only low crossing air masses, up to an altitude of 500 m amsl were considered for this analysis.

2.3.5 Satellite chlorophyll-a data and correlation analysis

The best estimate "Cloud Free" (Level-4) daily sea surface chlorophyll-a concentration (CHL; mg m^{-3}) data were downloaded from the EU Copernicus Marine Environment Monitoring Service (CMEMS; <http://marine.copernicus.eu/>) based on a multi-sensor approach (i.e., SeaWiFS, MODIS-Aqua, MERIS, VIIRS and OLCI-S3A). The Level-4 product is available globally at ~4 km spatial resolution. From this global dataset, CHL fields were extracted in the Arctic Ocean during summer 2018 to be merged with INPs data.

The relationship between INPs and phytoplankton biomass, in terms of CHL concentration, were investigated excluding the samples influenced by land inputs. The DFPC dataset was chosen to run this analysis because it provides a higher time-resolution than the WT-CRAFT one, and because it allows to differentiate between fine and coarse INPs. Each DFPC sample collected at a certain day has been considered as representative for that day, in order to be compared with the daily CHL time-series. The Pearson correlation coefficients between INPs and satellite-derived ocean color data, obtained by standard least squares regression, were computed at each grid point of the Arctic domain, and for different time-lags, to obtain the correlation maps presented in the results section.

2.3.6 Concentration weighted trajectory

The allocation of regional source areas potentially affecting INP concentrations sampled at Ny-Ålesund was achieved by applying the concentration weighted trajectory (CWT) model (Bycenkiene et al., 2014; Jeong et al., 2011; Hsu et al., 2003). In this procedure, each grid cell within the studied domain is associated to a weighted concentration, which is a measure of the source strength of a grid cell with respect to concentrations observed at the sampling site. The average weighted concentration in the grid cell (i,j) is determined as follows:

$$CWT_{ij} = \frac{\sum_{t=1}^L C_t D_{ijt}}{\sum_{t=1}^L D_{ijt}} \times W_{ij} \quad (1)$$



Where t is the index of the trajectory (arrival time simultaneous to INP samples), L is the total number of trajectories (5 days – hourly time step), C_t is the INP concentration observed at sampling location (receptor site) on arrival of trajectory t , and D_{ijt} is the residence time (time spent) of trajectory t in the grid cell (i,j). Given C_t for INP, D_{ijt} can be determined by counting the number of hourly trajectory segment endpoints in each grid cell for each trajectory. This was repeated for all the back trajectories L . A high value for CWT_{ij} means that air parcels traveling over the grid cell (i,j) would be, on average, associated with elevated concentrations at the receptor site.

In this study, five-day low (< 500 m) air mass back-trajectory corresponding to DFPC INP samples were utilized to produce the CWT spatial distribution. Similarly to the correlation analysis, the INP samples with a clear influence from land were excluded to consider only marine sources. The domain extends up to the limits of the area covered by the above described low back-trajectories (60° W – 30° E; 50° – 85° N) and was divided into $1^\circ \times 3^\circ$ latitude/longitude grid cells. The average number of endpoints over the grid cells with at least one endpoint (D^*) was 5.6. In order to avoid uncertainties that can occur due to grid cells containing a low number of endpoints, the CWT values were multiplied by a weighting factor (W_{ij}) as follows.

$$\begin{aligned} W_{ij} &= 1 && \text{if } D_{ij} \geq 2\bar{D} && (2) \\ 230 \quad W_{ij} &= 0.8 && \text{if } \bar{D} \leq D_{ij} < 2\bar{D} \\ W_{ij} &= 0.6 && \text{if } \bar{D}/2 \leq D_{ij} < \bar{D} \\ W_{ij} &= 0.4 && \text{if } D_{ij} < \bar{D}/2 \end{aligned}$$

3 Results

3.1 Comparison of DFPC and WT-CRAFT measurements

Figure 1 shows a comparison of the INP concentration ranges measured at Gruvebadet station, in spring-summer 2018 by the two deployed INP quantification techniques. While both measurements agree within one order of magnitude in terms of n_{INP} , an offset was observed between the two techniques. Specifically, n_{INP} measured in condensation mode (DFPC) resulted generally higher than those measured in immersion mode (WT-CRAFT) and the difference increased with the activation temperature. On average, $n_{\text{INP}}^{\text{DFPC}}$ was 3 times higher than $n_{\text{INP}}^{\text{WT-CRAFT}}$ at $T = -22^\circ\text{C}$ and 8 times higher at $T = -15^\circ\text{C}$. As a result, WT-CRAFT data presented a sharper $\Delta n_{\text{INP}}/\Delta T$ slope than the DFPC ones.

The observed offset may derive from the different time resolutions of the sampling for INP analyses, as well as from uncertainties in sampling activities and/or measurement uncertainties (Hiranuma et al., 2015; 2019). Conversely, it is also valid to assume a different sensitivity of Arctic INPs to different ice nucleation modes. Some previous studies presumed that condensation and immersion freezing are equivalent, but this hypothesis is questionable. Briefly, condensation freezing occurs if ice is formed immediately after water vapour condensation on the solid particle, followed by an additional ice growth by deposition. Unlike in condensation, a droplet must be formed at higher temperatures and necessarily undergoes supercooling



before freezing in immersion freezing (DeMott, 2002; Kanji et al., 2017). These different modalities could influence the obtained INP concentrations with the DFPC and the WT-CRAFT devices, particularly in case of mixed soluble/insoluble particles. Previous results, which evidenced a similar ice nucleating efficiency for immersion and condensation freezing, were indeed obtained with insoluble aerosol particles (Hiranuma et al., 2015; Wex et al., 2014). A detailed intercomparison of techniques is not the scope of this study. However, it is noteworthy that our past attempts to intercompare DFPC and WT-CRAFT measurements with different aerosol types yielded different results. For instance, microcrystalline and fibrous cellulose samples tended to form more ice crystals in the WT-CRAFT (Hiranuma et al., 2019), while ambient continental aerosol particles from the Po Valley resulted in equivalent or higher ice crystal numbers in the DFPC (unpublished). This suggests some sensitivity of the aerosol type to the different ice activation modalities deployed by the two instruments.

3.2 INP atmospheric concentration

INP concentrations (PM₁₀ size range) measured at Ny-Ålesund by DFPC during the spring campaign ranged 55-185 (median 115), 5-90 (53) and 3-37 (20) m⁻³, for T equal to -22, -18 and -15°C, respectively. During the summer campaign, the concentration ranges were 33-135 (median 77), 18-107 (45) and 6-66 (20) m⁻³, for the same activations temperatures (Figure 1).

WT-CRAFT measurements probed the immersion freezing ice nucleation ability of aerosol particles between 0 and -25°C (Figure 1). Above -9°C, no ice nucleation activity was observed in GVB samples. Between -9 and -14°C only a fraction of the samples (<50%) presented INP concentrations above the detection limit, with concentrations never above 3 m⁻³. In the rest of the temperature spectrum, *n*INP ranged 1-3 (median 2) m⁻³, at T = -14°C and 24-9082 (166) m⁻³, at T = -25°C.

The first ground level INP data reported in literature for Ny-Ålesund are those by Borys (1983). Measurements were performed with T between -28 and -16°C and the observed INP concentrations ranged between less than 10 to ca. 500 m⁻³. Later on, Bigg (1996) measured INP active at -15°C in a static chamber and at humidity just above 100%, during an icebreaker cruise to the North Pole (1 August – 6 October 1991). The overall geometric mean was 8.2±2.9 m⁻³ and the highest measured concentration was 250 m⁻³. The Ocean was the prevalent source of INPs. Similar measurements were performed by Bigg and Leck (2001) in the central Arctic ocean (20 July – 18 September 1996), resulting in median *n*INP ranging from 18 m⁻³, inside the ice pack, at the beginning of the expedition, to 1 m⁻³ at the end.

Subsequent measurements were performed in the immersion mode freezing. Conen et al. (2016) reported concentrations from 1.7 to about 10 m⁻³, at a coastal mountain observatory in Northern Norway (T=-15°C) Creamean et al. (2018) obtained INP concentrations in the range 5-10, 10-30 and 30-70 at T = -15, -20 and -25°C, respectively, in the Northern Alaskan Arctic during spring. The mean INP concentrations reported by Mason et al. (2016), at Alert station (Canada), ranged between 50 m⁻³ at -15°C and 990 m⁻³ at -25°C. Irish et al. (2019) measured INP concentrations, in the Canadian Arctic marine boundary layer during summer 2014, on board the CCGS Amudsen. Concentrations of INPs at -15, -20 and -25°C were 5, 44 and 154 m⁻³. Similarly, Si et al. (2018) reported average INP concentrations of 5±2, 20±4 and 186±40 m⁻³, for the same temperatures, at Alert station during March 2016. Given the great variability of parameters that intervene in the above reported INP



280 concentrations (instruments, locations, season, weather conditions, particle activation modality, etc...), we can conclude that the results of the present study are generally consistent with literature.

Both the datasets discussed in this work are in reasonable agreement with the results by Wex et al. (2019), that presented INP concentrations measured at the same station during spring and summer 2012. More in detail, at $T = -15^{\circ}\text{C}$, the DFPC data range covers the mid and upper part of the range of observations by Wex et al. (2019), while WT-CRAFT covers the lower part. Similarly, at $T = -18^{\circ}\text{C}$, the range of DFPC data overlaps well with the upper part of observations by Wex et al. (2019), while WT-CRAFT coincides with the lower part, even though our data span over a significantly wider range. At $T = -22^{\circ}\text{C}$, Wex et al. (2019) report a very narrow concentration range, while both our datasets, span a much wider range. It is worth considering that in Wex et al. (2019) the upper limit of observable INP concentration was set to some 10^{-2} L^{-1} (10 m^{-3}) depending on the volume of air sampled onto the analyzed filter portion. This may explain in part the wider range of the present observations with respect to the cited paper.

Previous DFPC measurements in remote conditions were performed at Mace Head (Ireland), during an intensive observation period in August 2015 (McCluskey et al., 2018b). Concentrations observed in carefully selected clean marine air masses ranged $0.4\text{-}15$ and $2\text{-}40 \text{ m}^{-3}$ for PM_1 and PM_{10} samples, respectively, which is about one order of magnitude lower than what observed at GVB in 2018. Similar concentrations were measured in parallel to the DFPC by an ice spectrometer (McCluskey et al., 2018). The significantly lower INP concentrations observed over the remote North Atlantic Ocean are likely due to the lack of continental particles, which we will show play an important role in the Arctic atmosphere (Sect. 3.7.2). If we compare with recent measurements performed at lower latitudes by DFPC $n\text{INP}$ over the Arctic was lower than those observed in continental European sites (Belosi et al., 2017; Rinaldi et al., 2017), but comparable or even higher with respect to those observed at high altitudes (Rinaldi et al., 2017) or at a Mediterranean coastal location (Rinaldi et al., 2019).

WT-CRAFT immersion freezing spectra ($n\text{INP}$ as a function of T) measured in the present study show a unique feature of ice nucleation behaviour at relatively high temperatures ($T > -20^{\circ}\text{C}$) in comparison to the freezing temperatures of other typical INPs (e.g., dust). Some spectra show initial nucleation at above -15°C and follow the previously reported ice nucleation spectral feature of marine biogenic aerosol particles (Wilson et al., 2015; Irish et al., 2017). For instance, the August #2 sample (highlighted in Figure 2) shows the bimodal activation with a hump feature at T above -15°C . The reason for early ice nucleation may be due to marine biogenic aerosols (Wilson et al., 2015; Irish et al., 2017). This aspect will be discussed in the next Sections.

3.3 Contribution of fine and coarse INPs

The sampling strategy adopted for DFPC measurements (parallel PM_1 and PM_{10} sampling) allowed a basic investigation of the INP size distribution. Table 1 reports the number concentrations of INPs measured in the two different size ranges, together with the average contribution of super-micrometer (coarse) INPs, derived by difference. A small contribution from coarse INPs characterized the spring campaign ($\sim 20\%$), suggesting that the dominant INP sources may be located at long distances, consistently with previous results (Shaw, 1995; Heidam et al., 1999; Stohl, 2006). During the summer campaign, a significant



($p < 0.005$) increase of the contribution of coarse INPs was observed (from ~50% at $T = -22^\circ\text{C}$ to ~70% at $T = -15^\circ\text{C}$), likely resulting from the activation of local sources after snow and ice melting. Furthermore, the increase of coarse INP contribution, from spring to summer time, is progressively more pronounced with increasing activation temperature, which may evidence the contribution of biological coarse particles during summer. This aspect agrees with the above considerations on the ice nucleation spectra from WT-CRAFT data. Similar results were reported by Mason et al. (2016) for Alert Arctic station, including the increasing coarse INPs contribution as a function of the activation temperature.

Si et al. (2018) and Creamen et al. (2018) reported a significant higher ice nucleation efficiency for super-micrometer particles sampled at Arctic stations. Similarly, comparing the INP number concentrations measured by DFPC in the fine and coarse modes with particle number concentration in the same size regimes (sub-micrometer: $3\text{--}61\text{ cm}^{-3}$; super-micrometer: $2\text{--}28\text{ cm}^{-3}$), a higher ice nucleation efficiency can be attributed to coarse particles during the summer campaign. In particular, the ice nucleation efficiency of coarse particle resulted from 1.7 (at $T = -22^\circ\text{C}$) to 5.5 (at $T = -15^\circ\text{C}$) times higher than that of fine particles. For comparison, a lower enhancement of the ice nucleation efficiency was observed for coarse particles with respect to fine ones in spring, with a maximum enhancement of 2.5 times at $T = -22^\circ\text{C}$ and negligible effect at lower temperatures.

3.4 Seasonality of the INP concentration

Recent works reported a marked seasonal trend for the INP concentration in the Arctic environment, with atmospheric loadings increasing from spring to summertime (Santl-Temkiv et al., 2019; Wex et al., 2019; Tobo et al., 2019). In particular, Wex et al. (2019) reported an INP concentration increase of the order of 10 times or more, at four Arctic sampling stations, including GVB. The paper deals with measurements from March 2012 to April 2016, but only data for spring-summer 2012 were available for GVB. The seasonal trend was explained assuming an important contribution from local sources, both of mineral and biological particles, during the warm season after ice and snow melting.

The time trends reported in Figure 3 do not show such a sharp seasonal increase in the INP atmospheric concentration from spring to summer. For DFPC data, actually, a significant ($p < 0.01$) n INP reduction (by a factor 1.5) was observed at $T = -22^\circ\text{C}$, passing from the spring campaign (April) to the summer period (July), while no significant ($p > 0.05$) differences were observed for $T = -15^\circ\text{C}$ and $T = -18^\circ\text{C}$. The time evolution of INP concentrations measured by WT-CRAFT agrees with the parallel dataset if we consider only the periods in which the two measurements were run in parallel: a significant ($p < 0.05$) reduction by a factor 1.6 is observed at -22°C and no significant differences can be appreciated at -15 and -18°C . On the other hand, considering the whole WT-CRAFT data extent, a statistically significant ($p < 0.5$) increasing n INP seasonal trend was observed only for temperatures within -17.5 and -21.5°C . Even in these cases, the spring-to-summer enhancement ratios never exceeded three-times. Conversely, it is worth noticing that a clear n INP peak was observed during June, at all temperatures lower than $T = -17^\circ\text{C}$, followed by a reduction of the concentrations to the same levels of April and May for the rest of the campaign. INP concentrations measured during June were averagely 1.7 ($T = -18^\circ\text{C}$) to 4.1 ($T = -22^\circ\text{C}$) times higher than what observed in the rest of the measurement period (excluding the last sample of the campaign).



345 The total particle number concentration in the 0.5-10 μm size range (the most INP-relevant; deMott et al., 2010) does not show any significant increase during June, which implies that aerosol particles were more ice active during that period (see Sect. 3.6 for more details). Another peak of INP concentration can be observed at the end of the WT-CRAFT measurement period, with the last sample presenting the highest concentrations of all the campaign for many activation temperatures. If this indicates an enhancement of the concentrations further on in the summer season we cannot tell, but we notice that the campaign extended
350 to half august, comprising the majority of the Arctic warm season.

In summary, during 2018 we observed different seasonal behaviours as a function of the considered activation temperature, with only INP active within a limited range of temperatures (-17.5 to -21.5°C) showing a statistical significant, but modest, seasonal trend, while particles active at temperatures below -17°C peaked mainly during the month of June. Conversely, the above cited previous observations at GVB (2012) showed a sharp increase (at least one order of magnitude) independently on
355 the probed activation temperatures. This discrepancy likely indicates that the inter-annual variability of meteorological and biogeochemical conditions determining the INP atmospheric concentration over the Arctic is wider and more complex than previously assumed. For sure, the number of observations in the Arctic and their temporal coverage are still too limited to derive general conclusions on the INP concentration trends.

3.5 Relation of $n\text{INP}$ with particle number concentration and meteorological parameters

360 Analyzing the patterns of the main meteorological parameters (T, P, RH and WS) in relation to $n\text{INP}$, no clear relation emerges, with the exception of precipitation events, which were often associated to a reduction of the INP concentration (Figure S2). The precipitation scavenging of aerosol particles (and consequently of INPs) by simple ice crystals and snowflakes (aggregate of ice crystals) was examined in the past both theoretically (Miller and Wang, 1989; Feng, 2009) and experimentally (Murakami et al., 1985; Zikova and Zdimal, 2016; Bell and Saunders, 1991). Kyrö et al. (2009) measured the snow scavenging coefficient
365 of sub-micrometer aerosol particles in the clean background SMEAR II station (Hyytiälä), using 4 years of particle number concentration spectra and meteorological parameters measurements. The obtained experimental median scavenging coefficient was found to be $1.8 \times 10^{-5} \text{ s}^{-1}$, varying between 0.87 and $5.2 \times 10^{-5} \text{ s}^{-1}$ in the 10 nm to 1 μm size range. Paramonov et al. (2011) reported an analysis of below-cloud snow scavenging of aerosols in the 0.01 to 1 μm size range for an urban environment, where the levels of air pollution were typically higher than at background sites. The calculated mean scavenging coefficients
370 varied between 6.65×10^{-6} and $5.14 \times 10^{-5} \text{ s}^{-1}$, in good agreement with those reported by Kyrö et al. (2009) for background conditions.

Although $n\text{INP}$ tends to covariate with particle number concentration (in the range 0.5-10 μm) during the spring campaign, no significant correlation was observed, for the DFPC dataset (with the only exception of $\text{INP}_{\text{PM}_{10}}$ at $T = -15^\circ\text{C}$). During summer, the lack of correlation between $n\text{INP}$ and particle number is even more accentuated. For WT-CRAFT significant correlations
375 ($p < 0.05$) were observed only for $T < -23^\circ\text{C}$ (temperatures not probed by the DFPC). Literature reports contrasting results about the correlation between INP and particle number concentration. A correlation is sometimes reported with the number concentration of aerosol particles larger than 0.5 μm (DeMott et al., 2010; DeMott et al., 2015; Mason et al., 2015; Schwikowski



et al., 1995). In other cases, a complete lack of correlation has been documented (Rogers et al., 1998; Richardson et al., 2007), which is not surprising considering that INPs are only a small fraction of total particles. Bigg et al. (1996) reported a good correlation between n_{INP} and accumulation mode particles, for one day of measurements over the high Arctic, while a modest but significant correlation ($R = 0.25 - 0.30$) between n_{INP} and particle number concentration in the 50-120 nm range was reported by Bigg et al. (2001), close to the North Pole. No other paper, to the best of our knowledge, addressed this issue in the Arctic environment.

3.6. Ice active site density (n_s)

Figure 4 presents the n_s distribution as a function of the activation temperature for the two datasets. DFPC showed a significant ($p < 0.05$) increase of the ice active site density (n_s), passing from the spring campaign to the summer period for all the probed activation temperatures (Figure 5). This result shows that the spring aerosol population, mainly related to long-range transport of anthropogenic aerosol particles from lower latitudes (Arctic haze), has a lower ability in nucleating ice than the summertime aerosol population, more related to local (Arctic) sources. This is in agreement with the findings by Hartmann et al. (2019), which showed a low impact of anthropogenic emissions over the INP concentration, with respect to the preindustrial period, through the analysis of ice core records. The spring-to-summer n_s increase is progressively more evident at $T = -15^\circ\text{C}$ than at $T = -22^\circ\text{C}$, suggesting that local aerosol particles are particularly efficient in nucleating ice at warmer temperatures, which is typical of biological INPs (Murray et al., 2012; Wilson et al., 2015; DeMott et al., 2016; McCluskey et al., 2018b).

Consistent results can be extrapolated from the WT-CRAFT data. Comparing the first month of the campaign, representative of spring conditions (16 April – 18 May) with the last month of the campaign, representative of full summer conditions (01 July – 02 August), an enhancement of n_s can be observed for all the activation temperatures, with the exception of the coldest one ($T = -25^\circ\text{C}$). This difference was significant ($p < 0.05$) for all the activation temperatures from -14 to -22°C , with the exception of $T = -16^\circ\text{C}$. Higher activation temperatures ($T < -14^\circ\text{C}$) were not considered because only a minority of samples ($< 50\%$) had an INP concentration above the detection limit at those temperatures. Differently from the DFPC data, the n_s increase as a function of the activation temperature had its maximum at $T = -19^\circ\text{C}$, with a sharp decrease towards higher and lower temperatures, with the minimum values obtained at $T = -25^\circ\text{C}$, where an actual n_s decrease was observed.

The time series of n_s values by WT-CRAFT reported in Figure 5 reflected the increase in INP concentration characterizing the month of June described above. This confirms that the enhancement in INP concentration (for $T < -17^\circ\text{C}$) observed in June was due to enhanced ice activity of the particle population, rather than to an increase of aerosol particle concentration.

In Figure 4, the ranges of n_s values observed at GVB are compared with the parameterizations by Niemand et al. (2012), for mineral dust, and McCluskey et al. (2018b), for marine aerosols. Furthermore, the n_s range of DFPC measurement performed in clean marine air masses, at Mace Head in 2015, are also reported. These measurements were performed in parallel with the ice spectrometer measurements used to derive the McCluskey et al. (2018) parameterization and show a substantial good agreement between the two instruments. The n_s values observed at GVB fell in between the two parameterizations, suggesting that the INP population over the Arctic in summer originates from a combination of mineral dust and marine aerosol particles.



A more detailed analysis of the relative contribution of mineral dust and marine aerosol sources during the study period will be presented in the following Sections.

3.7. Sources of INPs in the Arctic

3.7.1 Correlation with chemical tracers

415 In order to investigate the main sources of the INPs measured at GVB, a correlation analysis was performed between both
*n*INP datasets and the atmospheric concentration of chemical tracers routinely measured at the station. During the spring
campaign by DFPC, *n*INP_{DFPC} correlated, almost independently on the size fraction or the activation temperature, with tracers
of long range transported anthropogenic aerosol particles as nitrates, non-sea-salt-sulfate and non-sea-salt-potassium (Table
2). Indeed, Udisti et al. (2016) associated spring-time non-sea-salt-sulfate at GVB to anthropogenic sources, showing that the
420 production of biogenic non-sea-salt-sulfate from the sea is relevant only in summer-time. The results of the correlation analysis
are in line with the above considerations about long-range transport of anthropogenic aerosol during springtime over the Arctic.
A general tendency to anticorrelation with sodium and chlorine was also observed, even though significant values ($p < 0.05$)
were observed only in the PM₁ size fraction. Less clear indications resulted from the analysis of the summer DFPC data. The
only significant relations were observed for $T = -15^{\circ}\text{C}$: an anticorrelation was observed between *n*INP_{PM10} and particulate
425 mass, sea spray (sodium and chlorine) and mineral dust (calcium, magnesium and lithium) particles. Recently glacial soils
have been indicated as potentially important INP sources in the Arctic region during summertime (Tobo et al., 2019). If this
was true also during the DFPC measurement period, calcium, magnesium and lithium may be not the best chemical tracers for
this type of soils. Similarly, no clear source indications (no significant correlations) were derived from the correlation analysis
of the WT-CRAFT data (not shown).

430 3.7.2 Influence of ground conditions

The influence of ground conditions (sea-ice, snow, seawater and land) on low-travelling back-trajectories (<500m)
corresponding to the collected samples was evaluated by merging back trajectories and satellite ground type data (Wex et al.,
2019). Figure 6 shows that the contribution of the four considered ground types varies with the season. In spring, the majority
of contacts occurred with sea-ice or snow-covered land, while in summer low air masses were more influenced by ice-free
435 seawaters. The (snow-free) land contribution was the lowest in every season. Nevertheless, the influence of land sources on
the INP concentrations emerges clearly from Table 3 and Figure S3: air masses with a higher terrestrial influence were always
associated with *n*INP peaks. This is likely due to the higher ice nucleation efficiency of mineral dust and soil particles compared
to marine biological particles (Wilson et al., 2015; McCluskey et al., 2018a; McCluskey et al., 2018b). In summer, contacts
with snow-free land occurred mainly within the Svalbard archipelago (local sources) or over Greenland and Iceland (regional
440 sources), as shown by Figures S1. This outcome is in agreement with recent works pointing to both local and regional soils as
important INP sources over the Arctic (Tobo et al., 2019).



3.7.3 Contribution of marine biological INP sources

Considering that, during summer, the sampled air masses had ground contacts mainly over seawater, one can hypothesize that marine biological sources may dominate the INP concentration at GVB, outside the periods of elevated terrestrial influence.

445 To check this hypothesis, we investigated the spatio-temporal correlation of the INP datasets with satellite retrieved surface chlorophyll concentration, used as a tracer for marine biological activity, following the time-lag approach first introduced by Rinaldi et al. (2013). The DFPC dataset was selected to run this analysis because it provides a higher time resolution than the WT-CRAFT one and, most of all, because it allows to distinguish between fine and coarse INPs. In fact, McCluskey et al. (2018b) and Mansour et al. (2020a) showed that fine INPs tend to correlate better with chlorophyll in clean marine air masses.

450 To exclude interferences from land sources, we removed from the dataset the samples corresponding to back trajectories that have been in contact with land for more than 10% of the time (3 samples). Furthermore, we focused on INP data obtained at $T = -15^{\circ}\text{C}$, which are the most representative of ice nucleation by biological particles and the less subject to influences from mineral particles.

The results of the correlation analysis are reported in Figure 7, in the form of correlation maps. In the maps, the colour of each pixel represents the correlation coefficient (R) resulting from the linear regression between the CHL concentration in that pixel and $n\text{INP}_{\text{PM1}}$ measured at GVB. Different maps were obtained by considering different lag times between the two correlated time series, i.e., by considering CHL concentration values shifted back in times of 1 to 27 days with respect to the INP filter sampling times (the maps are shown in Figure S3). The lag time approach has been demonstrated to maximize the correlation between in situ coastal measurements of aerosol properties and CHL concentration fields (Rinaldi et al., 2013; Mansour et al., 2020a; Mansour et al., 2020b); it likely reflects the time scale of the biochemical processes responsible for the production of transferable organic matter in the seawater after the phytoplankton growing phase that is tracked by CHL patterns. Sea regions characterized by high correlation (red dots in the maps) are likely related to the emission of biological particles acting as INPs in our samples. Figure 7 reports two examples of correlation maps, with lag time 6 and 16 days. These maps were selected because they clearly show high correlation regions in the seawaters surrounding the Svalbard archipelago (lag time 6 days), close to the Greenland coast (lag time 16 days) and to the northeast of Iceland (lag time 16 days). These regions were all consistently located upwind GVB during the sampling period (Figure S1). All the obtained maps are available in the Supplementary Material, including those obtained with PM_{10} INP data, which as expected, do not evidence any significant correlation with CHL (Figure S4). In our interpretation, the lack of a correlation between surface CHL concentration and coarse INPs does not imply that coarse INPs are not emitted from the ocean surface, it simply evidences that CHL is not the appropriate proxy to track the emission of large biological INP from the oceans. Indeed, CHL has been previously observed to correlate with the enrichment of organic matter in sub-micron sea spray (Rinaldi et al., 2013; O'Dowd et al., 2015) but no investigation was ever attempted with super-micrometer particles. McCluskey et al. (2017) clearly evidenced the production of both sub- and super-micrometer INPs during laboratory experiments with controlled algal blooms, pointing out that different particle type and production mechanisms are involved.



475 Aware that the evidenced correlations alone cannot imply unambiguously a cause-effect relation, on the same INP dataset
(DFPC; PM₁; T = -15°; no land influenced samples) we run also the CWT spatial source attribution model. The resulting map
(Figure 7c) evidence that potential sub-micron INP sources at GVB, during the study period, were broadly located in the same
sea regions previously evidence by the spatio-temporal correlation with CHL. Furthermore, the CWT approach provides the
same results also with PM₁₀ data and independently on the considered activation temperature (Figure S5). The consistency of
480 the CWT source identification with those of the spatiotemporal correlation with CHL, two totally independent approaches,
suggests strongly that marine sources located between the Svalbard archipelago and Greenland/Iceland may have contributed
to the INP population measured at GVB during summer 2018, outside the major evidenced episodes of terrestrial influence.

4 Conclusions

Concentrations of INPs measured by two independent techniques at Ny-Alesund, during spring-summer 2018, were presented
485 in this work. The INP concentration trends obtained by the two techniques were qualitatively in good agreement, even though
with presence of a notable offset. However, the observed difference never exceeded one order of magnitude and we notice that
it increased with the activation temperature. This is presumably attributable to the different ice nucleation mechanisms probed
by the two techniques (condensation freezing, for DFPC, and immersion freezing, for WT-CRAFT), even though differences
in the sampling resolution and overall measurement uncertainties may also have contributed.

490 The INP concentration ranges reported in the present study are consistent with previous INP observations in the Arctic and at
Gruvebadet station, in particular. In agreement with previous works, the importance of super-micrometer INPs was evidenced
by the present study, particularly in summer and at relatively high activation temperatures. On the other hand, both datasets
lacked a clear seasonal trend, conversely to what has been recently reported by other investigators. The lack of a clear spring-
to-summer concentration increase in 2018, differently than what reported at the same station in 2012, likely reflects the inter-
495 annual variability of the conditions influencing INP emissions by local (Arctic) sources. Ny-Ålesund is located on the edge of
the Atlantic storm track, thereby, the site could be influenced by episodic particle transport from lower latitudes, open water,
local terrain or a combination of any. Thus, INP sources and composition, at this location, are inter-annually variable in nature.
Understanding whether the INP data from Ny-Ålesund would be representing the pan-Arctic conditions or a local situation
indeed requires long-term measurements. Our study presented in this paper might be an important step towards this broad
500 objective. Overall, our new study motivates and warrants the necessity for more frequent measurements on the long-term in
order to understand INP production processes in the Arctic environment.

Analysis of INP concentrations, active site density, low-travelling back-trajectories and ground conditions during the passage
of the air mass suggest that the summertime INP population may be contributed both by terrestrial and marine sources. When
the sampled air masses were influenced by contact with snow-free land, the INP concentration tended to peak, likely reflecting
505 the higher nucleation ability of terrestrial particles. Outside the major terrestrial inputs, the INP population was likely regulated
by marine INPs emitted from the sea surface. A prove of the relation between INP concentration (outside the major terrestrial



inputs) and the patterns of marine biological activity have been provided, suggesting that sources of INP may be located both in the seawaters surrounding the Svalbard archipelago and/or as far as Greenland and Iceland.

5 Data availability

510 Data discussed in this work are available at <http://dx.doi.org/10.17632/zf4wdcc3bw.1>
Satellite Chlorophyll data are available for download at <http://marine.copernicus.eu/> (product identifier: OCEANCOLOUR_GLO_CHL_L4_REP_OBSERVATIONS_009_082).

7 Author contribution

Conceptualization: MR, NH, FB; Formal Analysis: MR, NH, FB, KM; Investigation: GS, FB, CR, MM, DC, SB, RT, MP;
515 Methodology: GS, FB, NH; Writing: MR, FB, GS, NH.

8 Competing interests.

The authors declare that they have no conflict of interest.

9 Acknowledgements

The authors thank DSSSTA-CNR and its staff for the logistical support that allowed the realization of the experimental activity.
520 N. Hiranuma and C. A. Rodriguez acknowledges contributions of H.S. Vepuri, Y. Hou and Z. Salcido for their technical support on WT-CRAFT measurements. N. Hiranuma thanks for the funding support from Killgore Faculty Research Grant and the WTAMU's IoT and Research Computing program. N. Hiranuma also acknowledges partial financial support by Higher Education Assistance Fund (HEAF). This material is based upon work supported by the National Science Foundation under Grant No. 1941317 (CAREER: The Role of Ice-Nucleating Particles and Their Feedback on Clouds in Warming Arctic
525 Climate). The authors acknowledge the NySMAC, Ny-Ålesund Atmosphere Research Flagship Programme, for allowing the organization of a collaborative workshop meeting held in Bologna, Italy, in 2017. The workshop provided a venue for authors to come together that fostered this collaboration.



References

- 530 Becagli, S., Ghedini, C., Peeters, S., Rottiers, A., Traversi, R., Udisti, R., Chiari, M., Jalba, A., Despiau, S., Dayan, U., and
Temara, A.: MBAS (Methylene Blue Active Substances) and LAS (Linear Alkylbenzene Sulphonates) in Mediterranean
coastal aerosols: Sources and transport processes, *Atmospheric Environment*, 45, 6788-6801,
10.1016/j.atmosenv.2011.04.041, 2011.
- Bell, D. A., and Saunders, C. P. R.: THE SCAVENGING OF HIGH-ALTITUDE AEROSOL BY SMALL ICE CRYSTALS,
535 *Atmospheric Environment Part a-General Topics*, 25, 801-808, 1991.
- Belosi, F., Rinaldi, M., Decesari, S., Tarozzi, L., Nicosia, A., and Santachiara, G.: Ground level ice nuclei particle
measurements including Saharan dust events at a Po Valley rural site (San Pietro Capofiume, Italy), *Atmospheric Research*,
186, 116-126, 10.1016/j.atmosres.2016.11.012, 2017.
- Bigg, E. K., Mossop, S. C., Meade, R. T., and Thorndike, N. S. C.: The measurements of Ice Nuclei concentration by means
540 of Millipore filters, *Journal of applied meteorology*, 2, 266-269, 1963.
- Bigg, E. K.: Ice forming nuclei in the high Arctic, *Tellus Series B-Chemical and Physical Meteorology*, 48, 223-233,
10.1034/j.1600-0889.1996.t01-1-00007.x, 1996.
- Bigg, E. K., and Leck, C.: Cloud-active particles over the central Arctic Ocean, *Journal of Geophysical Research-Atmospheres*,
106, 32155-32166, 10.1029/1999jd901152, 2001.
- 545 Borys, R. D.: The effects of long-range transport of air pollutants on Arctic cloud-active aerosol, Thesis, Atmospheric Science
Paper No. 367, Colorado State University, Fort Collins, Colorado, USA, 1983.
- Borys, R. D.: STUDIES OF ICE NUCLEATION BY ARCTIC AEROSOL ON AGASP-II, *Journal of Atmospheric Chemistry*,
9, 169-185, 10.1007/bf00052831, 1989.
- Boucher, O., and Quaas, J.: Water vapour affects both rain and aerosol optical depth, *Nature Geoscience*, 6, 3-5,
550 10.1038/ngeo1692, 2013.
- Bycenkiene, S., Dudoitis, V., and Ulevicius, V.: The Use of Trajectory Cluster Analysis to Evaluate the Long-Range Transport
of Black Carbon Aerosol in the South-Eastern Baltic Region, *Advances in Meteorology*, 10.1155/2014/137694, 2014.
- Choi, Y. S., Lindzen, R. S., Ho, C. H., and Kim, J.: Space observations of cold-cloud phase change, *Proceedings of the National
Academy of Sciences of the United States of America*, 107, 11211-11216, 10.1073/pnas.1006241107, 2010.
- 555 Conen, F., Morris, C., Leifeld, J., Yakutin, M., and Alewell, C.: Biological residues define the ice nucleation properties of soil
dust, *Atmospheric Chemistry and Physics*, 11, 9643-9648, 10.5194/acp-11-9643-2011, 2011.
- Conen, F., Stopelli, E., and Zimmermann, L.: Clues that decaying leaves enrich Arctic air with ice nucleating particles,
Atmospheric Environment, 129, 91-94, 10.1016/j.atmosenv.2016.01.027, 2016.
- Cory, K., Mills, J., Tobo, Y., Murata, K., Goto-Azuma, K., Whiteside, C., McCauley, B., Bouma, C., and Hiranuma, N.:
560 Laboratory measurements of immersion freezing abilities of non-proteinaceous and proteinaceous biological particulate
proxies, *Earth and Space Science Open Archive*, DOI: <https://doi.org/10.1002/essoar.10500739.1>, 2019.



- Costa, A., Meyer, J., Afchine, A., Luebke, A., Gunther, G., Dorsey, J. R., Gallagher, M. W., Ehrlich, A., Wendisch, M., Baumgardner, D., Wex, H., and Kramer, M.: Classification of Arctic, midlatitude and tropical clouds in the mixed-phase temperature regime, *Atmospheric Chemistry and Physics*, 17, 12219-12238, 10.5194/acp-17-12219-2017, 2017.
- 565 Creamean, J. M., Kirpes, R. M., Pratt, K. A., Spada, N. J., Maahn, M., de Boer, G., Schnell, R. C., and China, S.: Marine and terrestrial influences on ice nucleating particles during continuous springtime measurements in an Arctic oilfield location, *Atmospheric Chemistry and Physics*, 18, 18023-18042, 10.5194/acp-18-18023-2018, 2018.
- Curry, J. A., Rossow, W. B., Randall, D., and Schramm, J. L.: Overview of Arctic cloud and radiation characteristics, *Journal of Climate*, 9, 1731-1764, 10.1175/1520-0442(1996)009<1731:ooacar>2.0.co;2, 1996.
- 570 DeMott, P. J.: Laboratory studies of cirrus cloud processes, in: *Cirrus*, edited by: Lynch, D. K., Sassen, K., Starr, D. O. C., and Stephens, G., Oxford University Press, New York, 102-135, 2002.
- DeMott, P. J., Prenni, A. J., Liu, X., Kreidenweis, S. M., Petters, M. D., Twohy, C. H., Richardson, M. S., Eidhammer, T., and Rogers, D. C.: Predicting global atmospheric ice nuclei distributions and their impacts on climate, *Proceedings of the National Academy of Sciences of the United States of America*, 107, 11217-11222, 10.1073/pnas.0910818107, 2010.
- 575 DeMott, P. J., Prenni, A. J., McMeeking, G. R., Sullivan, R. C., Petters, M. D., Tobo, Y., Niemand, M., Mohler, O., Snider, J. R., Wang, Z., and Kreidenweis, S. M.: Integrating laboratory and field data to quantify the immersion freezing ice nucleation activity of mineral dust particles, *Atmospheric Chemistry and Physics*, 15, 393-409, 10.5194/acp-15-393-2015, 2015.
- DeMott, P. J., Hill, T. C. J., McCluskey, C. S., Prather, K. A., Collins, D. B., Sullivan, R. C., Ruppel, M. J., Mason, R. H., Irish, V. E., Lee, T., Hwang, C. Y., Rhee, T. S., Snider, J. R., McMeeking, G. R., Dhaniyala, S., Lewis, E. R., Wentzell, J. J.
- 580 B., Abbatt, J., Lee, C., Sultana, C. M., Ault, A. P., Axson, J. L., Martinez, M. D., Venero, I., Santos-Figueroa, G., Stokes, M. D., Deane, G. B., Mayol-Bracero, O. L., Grassian, V. H., Bertram, T. H., Bertram, A. K., Moffett, B. F., and Franc, G. D.: Sea spray aerosol as a unique source of ice nucleating particles, *Proceedings of the National Academy of Sciences of the United States of America*, 113, 5797-5803, 10.1073/pnas.1514034112, 2016.
- DeMott, P. J., Mohler, O., Cziczo, D. J., Hiranuma, N., Petters, M. D., Petters, S. S., Belosi, F., Bingemer, H. G., Brooks, S.
- 585 D., Budke, C., Burkert-Kohn, M., Collier, K. N., Danielczok, A., Eppers, O., Felgitsch, L., Garimella, S., Grothe, H., Herenz, P., Hill, T. C. J., Hohler, K., Kanji, Z. A., Kiselev, A., Koop, T., Kristensen, T. B., Kruger, K., Kulkarni, G., Levin, E. J. T., Murray, B. J., Nicosia, A., O'Sullivan, D., Peckhaus, A., Polen, M. J., Price, H. C., Reicher, N., Rothenberg, D. A., Rudich, Y., Santachiara, G., Schiebel, T., Schrod, J., Seifried, T. M., Stratmann, F., Sullivan, R. C., Suski, K. J., Szakall, M., Taylor, H. P., Ullrich, R., Vergara-Temprado, J., Wagner, R., Whale, T. F., Weber, D., Welti, A., Wilson, T. W., Wolf, M. J., and
- 590 Zenker, J.: The Fifth International Workshop on Ice Nucleation phase 2 (FIN-02): laboratory intercomparison of ice nucleation measurements, *Atmospheric Measurement Techniques*, 11, 6231-6257, 10.5194/amt-11-6231-2018, 2018.
- Feng, J.: A size-resolved model for below-cloud scavenging of aerosols by snowfall, *Journal of Geophysical Research-Atmospheres*, 114, 10.1029/2008jd011012, 2009.
- Frohlich-Nowoisky, J., Hill, T. C. J., Pummer, B. G., Yordanova, P., Franc, G. D., and Poschl, U.: Ice nucleation activity in
- 595 the widespread soil fungus *Mortierella alpina*, *Biogeosciences*, 12, 1057-1071, 10.5194/bg-12-1057-2015, 2015.



- Garrett, T. J., Maestas, M. M., Krueger, S. K., and Schmidt, C. T.: Acceleration by aerosol of a radiative-thermodynamic cloud feedback influencing Arctic surface warming, *Geophysical Research Letters*, 36, 10.1029/2009gl040195, 2009.
- Giardi, F., Becagli, S., Traversi, R., Frosini, D., Severi, M., Caiazza, L., Ancillotti, C., Cappelletti, D., Moroni, B., Grotti, M., Bazzano, A., Lupi, A., Mazzola, M., Vitale, V., Abollino, O., Ferrero, L., Bolzacchini, E., Viola, A., and Udisti, R.: Size distribution and ion composition of aerosol collected at Ny-lesund in the spring-summer field campaign 2013, *Rendiconti Lincei-Scienze Fisiche E Naturali*, 27, 47-58, 10.1007/s12210-016-0529-3, 2016.
- 600 Goosse, H., Kay, J. E., Armour, K. C., Bodas-Salcedo, A., Chepfer, H., Docquier, D., Jonko, A., Kushner, P. J., Lecomte, O., Massonnet, F., Park, H. S., Pithan, F., Svensson, G., and Vancoppenolle, M.: Quantifying climate feedbacks in polar regions, *Nature Communications*, 9, 10.1038/s41467-018-04173-0, 2018.
- 605 Hartmann, M., Blunier, T., Brugger, S. O., Schmale, J., Schwikowski, M., Vogel, A., Wex, H., and Stratmann, F.: Variation of Ice Nucleating Particles in the European Arctic Over the Last Centuries, *Geophysical Research Letters*, 46, 4007-4016, 10.1029/2019gl082311, 2019.
- Heidam, N. Z., Wahlin, P., and Christensen, J. H.: Tropospheric gases and aerosols in northeast Greenland, *Journal of the Atmospheric Sciences*, 56, 261-278, 10.1175/1520-0469(1999)056<0261:tgaain>2.0.co;2, 1999.
- 610 Helfrich, S. R., McNamara, D., Ramsay, B. H., Baldwin, T., and Kasheta, T.: Enhancements to, and forthcoming developments in the Interactive Multisensor Snow and Ice Mapping System (IMS), *Hydrological Processes*, 21, 1576-1586, 10.1002/hyp.6720, 2007.
- Hiranuma, N., Mohler, O., Yamashita, K., Tajiri, T., Saito, A., Kiselev, A., Hoffmann, N., Hoose, C., Jantsch, E., Koop, T., and Murakami, M.: Ice nucleation by cellulose and its potential contribution to ice formation in clouds, *Nature Geoscience*, 8, 615 273-277, 10.1038/ngeo2374, 2015.
- Hiranuma, N., Adachi, K., Bell, D. M., Belosi, F., Beydoun, H., Bhaduri, B., Bingemer, H., Budke, C., Clemen, H. C., Conen, F., Cory, K. M., Curtius, J., DeMott, P. J., Eppers, O., Grawe, S., Hartmann, S., Hoffmann, N., Hohler, K., Jantsch, E., Kiselev, A., Koop, T., Kulkarni, G., Mayer, A., Murakami, M., Murray, B. J., Nicosia, A., Petters, M. D., Piazza, M., Polen, M., Reicher, N., Rudich, Y., Saito, A., Santachiara, G., Schiebel, T., Schill, G. P., Schneider, J., Segev, L., Stopelli, E., Sullivan, R. C., 620 Suski, K., Szakall, M., Tajiri, T., Taylor, H., Tobo, Y., Ullrich, R., Weber, D., Wex, H., Whale, T. F., Whiteside, C. L., Yamashita, K., Zelenyuk, A., and Mohler, O.: A comprehensive characterization of ice nucleation by three different types of cellulose particles immersed in water, *Atmospheric Chemistry and Physics*, 19, 4823-4849, 10.5194/acp-19-4823-2019, 2019.
- Hoose, C., and Moehler, O.: Heterogeneous ice nucleation on atmospheric aerosols: a review of results from laboratory experiments, *Atmospheric Chemistry and Physics*, 12, 9817-9854, 10.5194/acp-12-9817-2012, 2012.
- 625 Hsu, Y. K., Holsen, T. M., and Hopke, P. K.: Comparison of hybrid receptor models to locate PCB sources in Chicago, *Atmospheric Environment*, 37, 545-562, 10.1016/s1352-2310(02)00886-5, 2003.
- Ickes, L., Porter, G. C. E., Wagner, R., Adams, M. P., Bierbauer, S., Bertram, A. K., Bilde, M., Christiansen, S., Ekman, A. M. L., Gorokhova, E., Höhler, K., Kiselev, A. A., Leck, C., Möhler, O., Murray, B. J., Schiebel, T., Ullrich, R., and Salter, M.:



- Arctic marine ice nucleating aerosol: a laboratory study of microlayer samples and algal cultures, *Atmos. Chem. Phys. Discuss.*, <https://doi.org/10.5194/acp-2020-246>, 2020.
- 630 Irish, V. E., Elizondo, P., Chen, J., Chou, C., Charette, J., Lizotte, M., Ladino, L. A., Wilson, T. W., Gosselin, M., Murray, B. J., Polishchuk, E., Abbatt, J. P. D., Miller, L. A., and Bertram, A. K.: Ice-nucleating particles in Canadian Arctic sea-surface microlayer and bulk seawater, *Atmospheric Chemistry and Physics*, 17, 10583-10595, [10.5194/acp-17-10583-2017](https://doi.org/10.5194/acp-17-10583-2017), 2017.
- Irish, V. E., Hanna, S. J., Willis, M. D., China, S., Thomas, J. L., Wentzell, J. J. B., Cirisan, A., Si, M., Leitch, W. R., Murphy, J. G., Abbatt, J. P. D., Laskin, A., Girard, E., and Bertram, A. K.: Ice nucleating particles in the marine boundary layer in the Canadian Arctic during summer 2014, *Atmospheric Chemistry and Physics*, 19, 1027-1039, [10.5194/acp-19-1027-2019](https://doi.org/10.5194/acp-19-1027-2019), 2019.
- 635 Jeong, U., Kim, J., Lee, H., Jung, J., Kim, Y. J., Song, C. H., and Koo, J. H.: Estimation of the contributions of long range transported aerosol in East Asia to carbonaceous aerosol and PM concentrations in Seoul, Korea using highly time resolved measurements: a PSCF model approach, *Journal of Environmental Monitoring*, 13, 1905-1918, [10.1039/c0em00659a](https://doi.org/10.1039/c0em00659a), 2011.
- 640 Kanji, Z. A., Ladino, L. A., Wex, H., Boose, Y., Burkert-Kohn, M., Cziczo, D. J., and Kramer, M.: Overview of Ice Nucleating Particles, *Ice Formation and Evolution in Clouds and Precipitation: Measurement and Modeling Challenges*, 58, [10.1175/amsmonographs-d-16-0006.1](https://doi.org/10.1175/amsmonographs-d-16-0006.1), 2017.
- Kay, J. E., Raeder, K., Gettelman, A., and Anderson, J.: The Boundary Layer Response to Recent Arctic Sea Ice Loss and Implications for High-Latitude Climate Feedbacks, *Journal of Climate*, 24, 428-447, [10.1175/2010jcli3651.1](https://doi.org/10.1175/2010jcli3651.1), 2011.
- 645 Knopf, D., Alpert, P., Wang, B., and Aller, J.: Stimulation of ice nucleation by marine diatoms, *Nature Geoscience*, 4, 88-90, [10.1038/ngeo1037](https://doi.org/10.1038/ngeo1037)|[10.1038/NNGEO1037](https://doi.org/10.1038/NNGEO1037), 2011.
- Kyro, E. M., Gronholm, T., Vuollekoski, H., Virkkula, A., Kulmala, M., and Laakso, L.: Snow scavenging of ultrafine particles: field measurements and parameterization, *Boreal Environment Research*, 14, 527-538, 2009.
- Lee, L. A., Reddington, C. L., and Carslaw, K. S.: On the relationship between aerosol model uncertainty and radiative forcing uncertainty, *Proceedings of the National Academy of Sciences of the United States of America*, 113, 5820-5827, [10.1073/pnas.1507050113](https://doi.org/10.1073/pnas.1507050113), 2016.
- 650 Lohmann, U.: A glaciation indirect aerosol effect caused by soot aerosols, *Geophysical Research Letters*, 29, [10.1029/2001gl014357](https://doi.org/10.1029/2001gl014357), 2002.
- Lupi, A., Busetto, M., Becagli, S., Giardi, F., Lanconelli, C., Mazzola, M., Udisti, R., Hansson, H. C., Henning, T., Petkov, B., Strom, J., Krejci, R., Tunved, P., Viola, A. P., and Vitale, V.: Multi-seasonal ultrafine aerosol particle number concentration measurements at the Gruvebadet observatory, Ny-lesund, Svalbard Islands, *Rendiconti Lincei-Scienze Fisiche E Naturali*, 27, 59-71, [10.1007/s12210-016-0532-8](https://doi.org/10.1007/s12210-016-0532-8), 2016.
- 655 Mansour, K., Decesari, S., Facchini, M. C., Belosi, F., Paglione, M., Sandrini, S., Bellacicco, M., Marullo, S., Santolero, R., Ovadnevaite, J., Ceburnis, D., O'Dowd, C.D., Roberts, G., Sanchez, K., and Rinaldi, M.: Linking marine biological activity to aerosol chemical composition and cloud-relevant properties over the North Atlantic Ocean. *Journal of Geophysical Research: Atmospheres*, 125, e2019JD032246. <https://doi.org/10.1029/2019JD032246>, 2020a.



- Mansour, K., Decesari, S., Bellacicco, M., Marullo, S., Santolero, R., Bonasoni, P., Facchini, M. C., Ovadnevaite, J., Ceburnis, D., O'Dowd, C., and Rinaldi, M.: Particulate methanesulfonic acid over the central Mediterranean Sea: Source region identification and relationship with phytoplankton activity, *Atmospheric Research*, 237, 10.1016/j.atmosres.2019.104837, 2020b.
- Mason, R. H., Si, M., Li, J., Chou, C., Dickie, R., Toom-Sauntry, D., Pohlker, C., Yakobi-Hancock, J. D., Ladino, L. A., Jones, K., Leaitch, W. R., Schiller, C. L., Abbatt, J. P. D., Huffman, J. A., and Bertram, A. K.: Ice nucleating particles at a coastal marine boundary layer site: correlations with aerosol type and meteorological conditions, *Atmospheric Chemistry and Physics*, 15, 12547-12566, 10.5194/acp-15-12547-2015, 2015.
- Mason, R. H., Si, M., Chou, C., Irish, V. E., Dickie, R., Elizondo, P., Wong, R., Brintnell, M., Elsasser, M., Lassar, W. M., Pierce, K. M., Leaitch, W. R., MacDonald, A. M., Platt, A., Toom-Sauntry, D., Sarda-Esteve, R., Schiller, C. L., Suski, K. J., Hill, T. C. J., Abbatt, J. P. D., Huffman, J. A., DeMott, P. J., and Bertram, A. K.: Size-resolved measurements of ice-nucleating particles at six locations in North America and one in Europe, *Atmospheric Chemistry and Physics*, 16, 1637-1651, 10.5194/acp-16-1637-2016, 2016.
- Mazzola, M., Viola, A. P., Lanconelli, C., and Vitale, V.: Atmospheric observations at the Amundsen-Nobile Climate Change Tower in Ny-lesund, Svalbard, *Rendiconti Lincei-Scienze Fisiche E Naturali*, 27, 7-18, 10.1007/s12210-016-0540-8, 2016.
- McCluskey, C. S., Hill, T. C. J., Malfatti, F., Sultana, C. M., Lee, C., Santander, M. V., Beall, C. M., Moore, K. A., Cornwell, G. C., Collins, D. B., Prather, K. A., Jayarathne, T., Stone, E. A., Azam, F., Kreidenweis, S. M., and DeMott, P. J.: A Dynamic Link between Ice Nucleating Particles Released in Nascent Sea Spray Aerosol and Oceanic Biological Activity during Two Mesocosm Experiments, *Journal of the Atmospheric Sciences*, 74, 151-166, 10.1175/jas-d-16-0087.1, 2017.
- McCluskey, C. S., Hill, T. C. J., Sultana, C. M., Laskina, O., Trueblood, J., Santander, M. V., Beall, C. M., Michaud, J. M., Kreidenweis, S. M., Prather, K. A., Grassian, V., and DeMott, P. J.: A Mesocosm Double Feature: Insights into the Chemical Makeup of Marine Ice Nucleating Particles, *Journal of the Atmospheric Sciences*, 75, 2405-2423, 10.1175/jas-d-17-0155.1, 2018a.
- McCluskey, C. S., Ovadnevaite, J., Rinaldi, M., Atkinson, J., Belosi, F., Ceburnis, D., Marullo, S., Hill, T. C. J., Lohmann, U., Kanji, Z. A., O'Dowd, C., Kreidenweis, S. M., and DeMott, P. J.: Marine and Terrestrial Organic Ice-Nucleating Particles in Pristine Marine to Continentally Influenced Northeast Atlantic Air Masses, *Journal of Geophysical Research-Atmospheres*, 123, 6196-6212, 10.1029/2017jd028033, 2018b.
- Miller, N. L., and Wang, P. K.: THEORETICAL DETERMINATION OF THE EFFICIENCY OF AEROSOL-PARTICLE COLLECTION BY FALLING COLUMNAR ICE CRYSTALS, *Journal of the Atmospheric Sciences*, 46, 1656-1663, 10.1175/1520-0469(1989)046<1656:tdoteo>2.0.co;2, 1989.
- Morrison, H., de Boer, G., Feingold, G., Harrington, J., Shupe, M. D., and Sulia, K.: Resilience of persistent Arctic mixed-phase clouds, *Nature Geoscience*, 5, 11-17, 10.1038/ngeo1332, 2012.



- Murakami, M., Kikuchi, K., and Magono, C.: EXPERIMENTS ON AEROSOL SCAVENGING BY NATURAL SNOW
695 CRYSTALS .1. COLLECTION EFFICIENCY OF UNCHARGED SNOW CRYSTALS FOR MICRON AND SUB-
MICRON PARTICLES, *Journal of the Meteorological Society of Japan*, 63, 119-129, 10.2151/jmsj1965.63.1_119, 1985.
- Murray, B. J., O'Sullivan, D., Atkinson, J. D., and Webb, M. E.: Ice nucleation by particles immersed in supercooled cloud
droplets, *Chemical Society Reviews*, 41, 6519-6554, 10.1039/c2cs35200a, 2012.
- National Ice-Center, U. S.: IMS Daily Northern Hemisphere Snow and Ice Analysis at 1 km, 4 km, and 24 km Resolutions,
700 Version 1. In: updated daily, Boulder , Colorado USA. NSIDC: National Snow and Ice Data Center, 2008.
- Niemand, M., Mohler, O., Vogel, B., Vogel, H., Hoose, C., Connolly, P., Klein, H., Bingemer, H., DeMott, P., Skrotzki, J.,
and Leisner, T.: A Particle-Surface-Area-Based Parameterization of Immersion Freezing on Desert Dust Particles, *Journal of
the Atmospheric Sciences*, 69, 3077-3092, 10.1175/jas-d-11-0249.1, 2012.
- O'Dowd, C., Ceburnis, D., Ovadnevaite, J., Bialek, J., Stengel, D. B., Zacharias, M., Nitschke, U., Connan, S., Rinaldi, M.,
705 Fuzzi, S., Decesari, S., Facchini, M. C., Marullo, S., Santolero, R., Dell'Anno, A., Corinaldesi, C., Tangherlini, M., and
Danovaro, R.: Connecting marine productivity to sea-spray via nanoscale biological processes: Phytoplankton Dance or Death
Disco?, *Scientific Reports*, 5, 10.1038/srep14883, 2015.
- O'Sullivan, D., Murray, B. J., Malkin, T. L., Whale, T. F., Umo, N. S., Atkinson, J. D., Price, H. C., Baustian, K. J., Browse,
J., and Webb, M. E.: Ice nucleation by fertile soil dusts: relative importance of mineral and biogenic components, *Atmospheric
710 Chemistry and Physics*, 14, 1853-1867, 10.5194/acp-14-1853-2014, 2014.
- O'Sullivan, D., Murray, B. J., Ross, J. F., Whale, T. F., Price, H. C., Atkinson, J. D., Umo, N. S., and Webb, M. E.: The
relevance of nanoscale biological fragments for ice nucleation in clouds, *Scientific Reports*, 5, 10.1038/srep08082, 2015.
- Paramonov, M., Gronholm, T., and Virkkula, A.: Below-cloud scavenging of aerosol particles by snow at an urban site in
Finland, *Boreal Environment Research*, 16, 304-320, 2011.
- 715 Pithan, F., and Mauritsen, T.: Arctic amplification dominated by temperature feedbacks in contemporary climate models,
Nature Geoscience, 7, 181-184, 10.1038/ngeo2071, 2014.
- Prenni, A. J., Harrington, J. Y., Tjernstrom, M., DeMott, P. J., Avramov, A., Long, C. N., Kreidenweis, S. M., Olsson, P. Q.,
and Verlinde, J.: Can ice-nucleating aerosols affect arctic seasonal climate?, *Bulletin of the American Meteorological Society*,
88, 541-+, 10.1175/bams-88-4-541, 2007.
- 720 Richardson, M. S., DeMott, P. J., Kreidenweis, S. M., Cziczo, D. J., Dunlea, E. J., Jimenez, J. L., Thomson, D. S., Ashbaugh,
L. L., Borys, R. D., Westphal, D. L., Casuccio, G. S., and Lersch, T. L.: Measurements of heterogeneous ice nuclei in the
western United States in springtime and their relation to aerosol characteristics, *Journal of Geophysical Research-Atmospheres*,
112, 10.1029/2006jd007500, 2007.
- Rinaldi, M., Fuzzi, S., Decesari, S., Marullo, S., Santolero, R., Provenzale, A., von Hardenberg, J., Ceburnis, D., Vaishya, A.,
725 O'Dowd, C. D., and Facchini, M. C.: Is chlorophyll-a the best surrogate for organic matter enrichment in submicron primary
marine aerosol?, *Journal of Geophysical Research-Atmospheres*, 118, 4964-4973, 10.1002/jgrd.50417, 2013.



- Rinaldi, M., Santachiara, G., Nicosia, A., Piazza, M., Decesari, S., Gilardoni, S., Paglione, M., Cristofanelli, P., Marinoni, A., Bonasoni, P., and Belosi, F.: Atmospheric Ice Nucleating Particle measurements at the high mountain observatory Mt. Cimone (2165 m a.s.l., Italy), *Atmospheric Environment*, 171, 173-180, 10.1016/j.atmosenv.2017.10.027, 2017.
- 730 Rinaldi, M., Nicosia, A., Santachiara, G., Piazza, M., Paglione, M., Gilardoni, S., Sandrini, S., Cristofanelli, P., Marinoni, A., Bonasoni, P., Facchini, M. C., and Belosi, F.: Ground level ice nucleating particles measurements at Capo Granitola, a Mediterranean coastal site, *Atmospheric Research*, 219, 57-64, 10.1016/j.atmosres.2018.12.022, 2019.
- Rogers, D. C., DeMott, P. J., Kreidenweis, S. M., and Chen, Y. L.: Measurements of ice nucleating aerosols during SUCCESS, *Geophysical Research Letters*, 25, 1383-1386, 10.1029/97gl03478, 1998.
- 735 Rolph, G., Stein, A., and Stunder, B.: Real-time Environmental Applications and Display sYstem: READY, *Environmental Modelling & Software*, 95, 210-228, 10.1016/j.envsoft.2017.06.025, 2017.
- Santachiara, G., Di Matteo, L., Prodi, F., and Belosi, F.: Atmospheric particles acting as Ice Forming Nuclei in different size ranges, *Atmospheric Research*, 96, 266-272, 10.1016/j.atmosres.2009.08.004, 2010.
- Santl-Temkiv, T., Lange, R., Beddows, D., Rauter, U., Pilgaard, S., Dall'Osto, M., Gunde-Cimerman, N., Massling, A., and Wex, H.: Biogenic Sources of Ice Nucleating Particles at the High Arctic Site Villum Research Station, *Environmental Science & Technology*, 53, 10580-10590, 10.1021/acs.est.9b00991, 2019.
- Schrod, J., Weber, D., Thomson, E. S., Pöhlker, C., Saturno, J., Artaxo, P., Curtius, J., and Bingemer, H.: Ice nucleating particles from a large-scale sampling network: insight into geographic and temporal variability, *EGU General Assembly, Vienna, Austria*, 23-28 April 2017, EGU2017-13773, 2017.
- 745 Schwikowski, M., Seibert, P., Baltensperger, U., and Gaggeler, H. W.: A STUDY OF AN OUTSTANDING SAHARAN DUST EVENT AT THE HIGH-ALPINE SITE JUNGFRAUJOCH, SWITZERLAND, *Atmospheric Environment*, 29, 1829-1842, 10.1016/1352-2310(95)00060-c, 1995.
- Shaw, G. E.: The arctic haze phenomenon, *Bulletin of the American Meteorological Society*, 76, 2403-2413, 10.1175/1520-0477(1995)076<2403:tahp>2.0.co;2, 1995.
- 750 Shupe, M. D., Matrosov, S. Y., and Uttal, T.: Arctic mixed-phase cloud properties derived from surface-based sensors at SHEBA, *Journal of the Atmospheric Sciences*, 63, 697-711, 10.1175/jas3659.1, 2006.
- Shupe, M. D., Walden, V. P., Eloranta, E., Uttal, T., Campbell, J. R., Starkweather, S. M., and Shiobara, M.: Clouds at Arctic Atmospheric Observatories. Part I: Occurrence and Macrophysical Properties, *Journal of Applied Meteorology and Climatology*, 50, 626-644, 10.1175/2010jamc2467.1, 2011.
- 755 Si, M., Irish, V. E., Mason, R. H., Vergara-Temprado, J., Hanna, S. J., Ladino, L. A., Yakobi-Hancock, J. D., Schiller, C. L., Wentzell, J. J. B., Abbatt, J. P. D., Carslaw, K. S., Murray, B. J., and Bertram, A. K.: Ice-nucleating ability of aerosol particles and possible sources at three coastal marine sites, *Atmospheric Chemistry and Physics*, 18, 15669-15685, 10.5194/acp-18-15669-2018, 2018.



- 760 Solomon, A., de Boer, G., Creamean, J. M., McComiskey, A., Shupe, M. D., Maahn, M., and Cox, C.: The relative impact of cloud condensation nuclei and ice nucleating particle concentrations on phase partitioning in Arctic mixed-phase stratocumulus clouds, *Atmospheric Chemistry and Physics*, 18, 17047-17059, 10.5194/acp-18-17047-2018, 2018.
- Stein, A. F., Draxler, R. R., Rolph, G. D., Stunder, B. J. B., Cohen, M. D., and Ngan, F.: NOAA'S HYSPLIT ATMOSPHERIC TRANSPORT AND DISPERSION MODELING SYSTEM, *Bulletin of the American Meteorological Society*, 96, 2059-2077, 10.1175/bams-d-14-00110.1, 2015.
- 765 Stocker, T. F., Qin, D., Plattner, G. K., Tignor, M., Allen, S. K., Boschung, J., Nauels, A., Xia, Y., Bex, V. and Midgley, P. M.: Climate change 2013: The physical science basis." Contribution of working group I to the fifth assessment report of the intergovernmental panel on climate change", edited, Cambridge University Press, 2013.
- Stohl, A.: Characteristics of atmospheric transport into the Arctic troposphere, *Journal of Geophysical Research-Atmospheres*, 111, 10.1029/2005jd006888, 2006.
- 770 Tesson, S. V. M., and Santl-Temkiv, T.: Ice Nucleation Activity and Aeolian Dispersal Success in Airborne and Aquatic Microalgae, *Frontiers in Microbiology*, 9, 10.3389/fmicb.2018.02681, 2018.
- Tobo, Y.: An improved approach for measuring immersion freezing in large droplets over a wide temperature range, *Scientific Reports*, 6, 10.1038/srep32930, 2016.
- Tobo, Y., Adachi, K., DeMott, P. J., Hill, T. C. J., Hamilton, D. S., Mahowald, N. M., Nagatsuka, N., Ohata, S., Uetake, J., Kondo, Y., and Koike, M.: Glacially sourced dust as a potentially significant source of ice nucleating particles, *Nature Geoscience*, 12, 253+, 10.1038/s41561-019-0314-x, 2019.
- 775 Udisti, R., Bazzano, A., Becagli, S., Bolzacchini, E., Caiazza, L., Cappelletti, D., Ferrero, L., Frosini, D., Giardi, F., Grotti, M., Lupi, A., Malandrino, M., Mazzola, M., Moroni, B., Severi, M., Traversi, R., Viola, A., and Vitale, V.: Sulfate source apportionment in the Ny-Alesund (Svalbard Islands) Arctic aerosol, *Rendiconti Lincei-Scienze Fisiche E Naturali*, 27, 85-94, 10.1007/s12210-016-0517-7, 2016.
- 780 Vali, G.: ICE NUCLEATION WORKSHOP, 1975 LARAMIE, WYOMING, 19 MAY - 6 JUNE 1975, *Bulletin of the American Meteorological Society*, 56, 1180-1184, 1975.
- Wang, X. F., Sultana, C. M., Trueblood, J., Hill, T. C. J., Malfatti, F., Lee, C., Laskina, O., Moore, K. A., Beall, C. M., McCluskey, C. S., Cornwell, G. C., Zhou, Y. Y., Cox, J. L., Pendergraft, M. A., Santander, M. V., Bertram, T. H., Cappa, C. D., Azam, F., DeMott, P. J., Grassian, V. H., and Prather, K. A.: Microbial Control of Sea Spray Aerosol Composition: A Tale of Two Blooms, *Acs Central Science*, 1, 124-131, 10.1021/acscentsci.5b00148, 2015.
- 785 Wex, H., DeMott, P. J., Tobo, Y., Hartmann, S., Rosch, M., Clauss, T., Tomsche, L., Niedermeier, D., and Stratmann, F.: Kaolinite particles as ice nuclei: learning from the use of different kaolinite samples and different coatings, *Atmospheric Chemistry and Physics*, 14, 5529-5546, 10.5194/acp-14-5529-2014, 2014.
- 790 Wex, H., Huang, L., Zhang, W., Hung, H., Traversi, R., Becagli, S., Sheesley, R. J., Moffett, C. E., Barrett, T. E., Bossi, R., Skov, H., Hunerbein, A., Lubitz, J., Löffler, M., Linke, O., Hartmann, M., Herenz, P., and Stratmann, F.: Annual variability



- of ice-nucleating particle concentrations at different Arctic locations, *Atmospheric Chemistry and Physics*, 19, 5293-5311, 10.5194/acp-19-5293-2019, 2019.
- Whiteside, C., Tobo, Y., Brooks, S., Mulamba, O., Mirrielees, J., and Hiranuma, N.: Immersion freezing of coal combustion ash particles from the Texas Panhandle, *Earth and Space Science Open Archive*, DOI: <https://doi.org/10.1002/essoar.10500578.1>, 2019.
- Wilson, T. W., Ladino, L. A., Alpert, P. A., Breckels, M. N., Brooks, I. M., Browse, J., Burrows, S. M., Carslaw, K. S., Huffman, J. A., Judd, C., Kilhau, W. P., Mason, R. H., McFiggans, G., Miller, L. A., Najera, J. J., Polishchuk, E., Rae, S., Schiller, C. L., Si, M., Temprado, J. V., Whale, T. F., Wong, J. P. S., Wurl, O., Yakobi-Hancock, J. D., Abbatt, J. P. D., Aller, J. Y., Bertram, A. K., Knopf, D. A., and Murray, B. J.: A marine biogenic source of atmospheric ice-nucleating particles, *Nature*, 525, 234-+, 10.1038/nature14986, 2015.
- Zikova, N., and Zdimal, V.: Precipitation scavenging of aerosol particles at a rural site in the Czech Republic, *Tellus Series B-Chemical and Physical Meteorology*, 68, 10.3402/tellusb.v68.27343, 2016.



805 **Table 1: Average (\pm standard deviation) and median (in brackets) INP concentrations measured at GVB during 2018.**

		-22°C			-18°C			-15°C		
		PM ₁	PM ₁₀	Coarse contrib.	PM ₁	PM ₁₀	Coarse contrib.	PM ₁	PM ₁₀	Coarse contrib.
		m ⁻³	m ⁻³	%	m ⁻³	m ⁻³	%	m ⁻³	m ⁻³	%
DFPC	Spring	97±48 (85)	116±42 (115)	21±22 (20)	45±25 (49)	55±28 (53)	20±20 (17)	13±9 (14)	18±9 (20)	32±36 (22)
	Summer	43±27 (38)	74±26 (77)	45±24 (48)	23±13 (23)	50±22 (47)	53±17 (58)	9±9 (7)	24±14 (20)	65±23 (72)
WT-CRAFT		-	39±45 (26)	-	-	8±7 (6)	-	-	3±1 (2)	-



810 **Table 2a: Correlations of INP concentrations, for PM₁ and PM₁₀ samples by DFPC, with chemical tracers during the spring campaign. Values reported in bold are statistically significant (p<0.05).**

	-22°C		-18°C		-15°C	
	PM ₁	PM ₁₀	PM ₁	PM ₁₀	PM ₁	PM ₁₀
PM ₁₀ mass	0.00	0.13	0.12	0.28	0.21	0.49
Na ⁺	-0.61	-0.49	-0.59	-0.36	-0.60	-0.25
Mg ⁺²	-0.52	-0.32	-0.38	-0.10	-0.43	-0.03
Ca ⁺²	0.25	0.45	0.24	0.27	0.34	0.64
Cl ⁻	-0.64	-0.51	-0.64	-0.42	-0.65	-0.30
NO ₃ ⁻	0.61	0.59	0.67	0.73	0.72	0.54
MSA	-0.26	-0.28	-0.42	-0.52	-0.40	-0.65
Li ⁺	-0.36	-0.22	-0.29	-0.11	-0.22	0.06
nssSO ₄ ⁻²	0.43	0.44	0.53	0.43	0.62	0.67
nssK ⁺	0.60	0.56	0.68	0.56	0.77	0.72

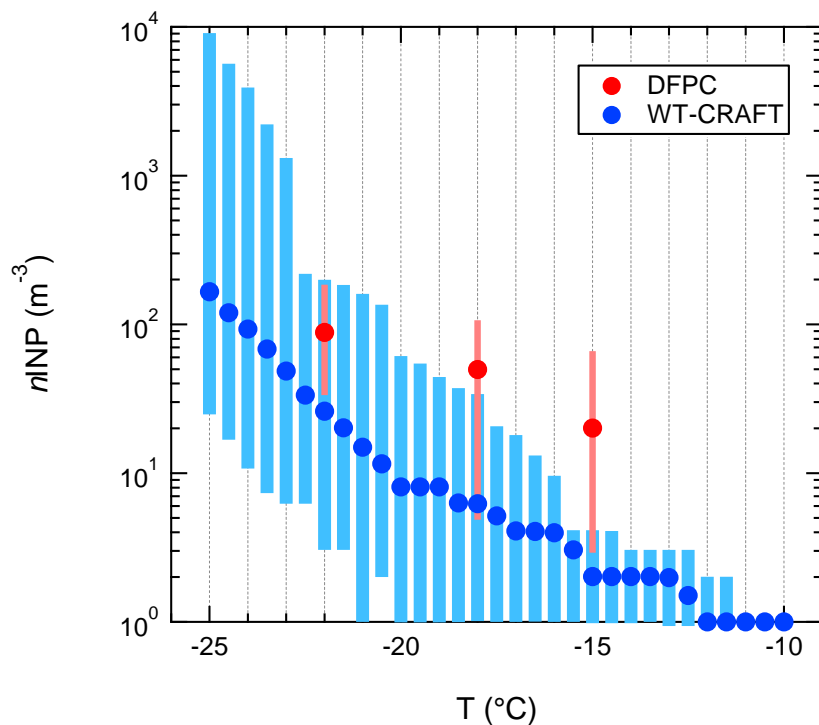
Table 2b: Correlations of INP concentrations, for PM₁ and PM₁₀ samples by DFPC, with chemical tracers during the summer campaign. Values reported in bold are statistically significant (p<0.05).

	-22		-18		-15	
	PM ₁	PM ₁₀	PM ₁	PM ₁₀	PM ₁	PM ₁₀
PM ₁₀ mass	-0.07	-0.27	-0.29	-0.35	-0.32	-0.49
Na ⁺	-0.16	-0.36	-0.39	-0.43	-0.31	-0.52
Mg ⁺²	-0.12	-0.35	-0.41	-0.48	-0.35	-0.57
Ca ⁺²	-0.17	-0.33	-0.42	-0.44	-0.30	-0.55
Cl ⁻	-0.15	-0.38	-0.37	-0.45	-0.28	-0.51
NO ₃ ⁻	0.05	0.02	-0.27	-0.17	-0.33	-0.36
MSA	0.15	-0.11	-0.27	-0.24	-0.28	-0.37
Li ⁺	-0.16	-0.32	-0.37	-0.42	-0.35	-0.49
nssSO ₄ ⁻²	0.08	-0.02	-0.27	-0.18	-0.21	-0.32
nssK ⁺	0.36	0.31	0.13	0.21	0.16	0.21

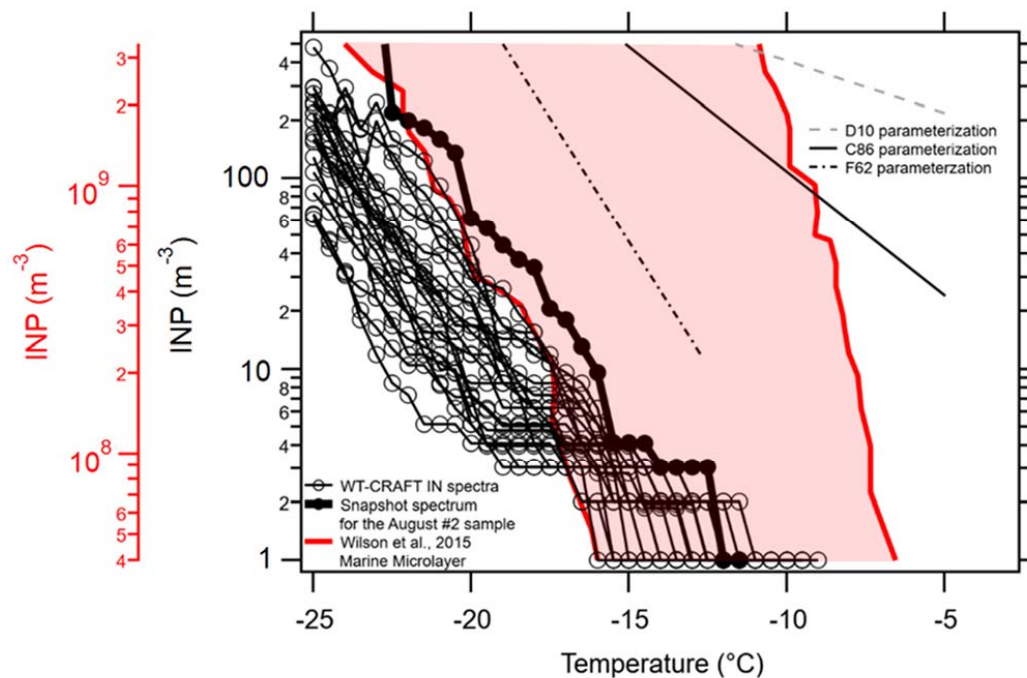


Table 3: Correlation coefficient (R) resulting from the linear regression between n INP (at T = -15, -18 and -22°C) and the contribution of the four considered ground types. Values reported in bold are statistically significant ($p < 0.05$).

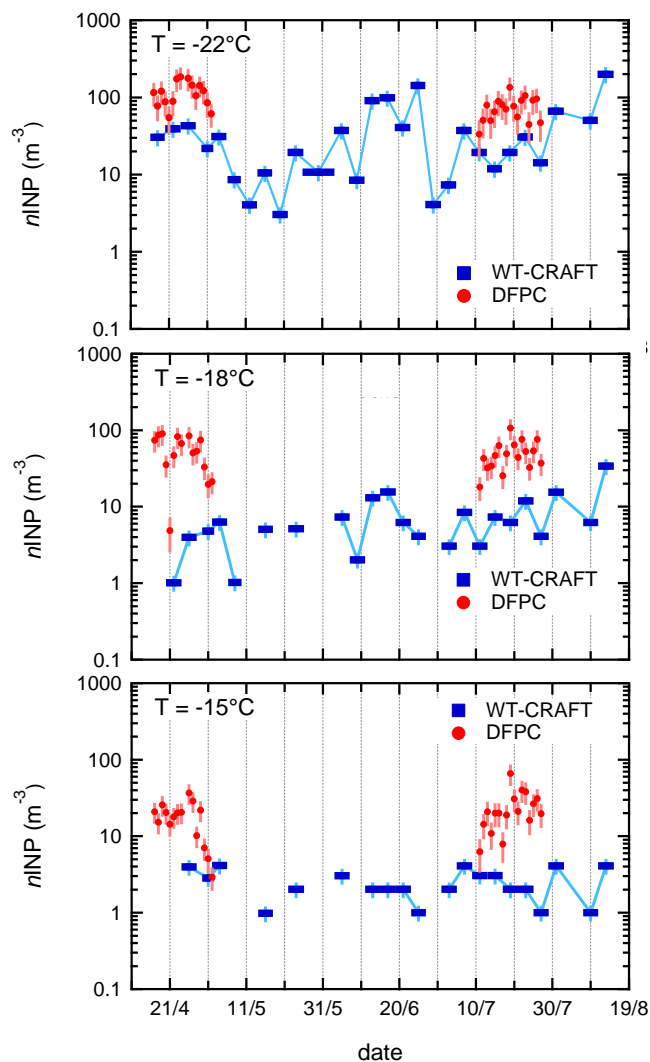
	DFPC_spring		
	INP_-15	INP-18	INP-22
Sea-Water	-0.63	-0.54	-0.39
Land	-0.05	0.36	-0.25
Sea-Ice	0.24	0.16	0.08
Snow	0.23	0.18	0.25
	DFPC_summer		
	INP_-15	INP-18	INP-22
Sea-Water	-0.60	-0.43	-0.48
Land	0.86	0.72	0.65
Sea-Ice	-0.15	-0.24	-0.11
Snow	0.39	0.32	0.33
	WT-CRAFT		
	INP_-15	INP-18	INP-22
Sea-Water	-0.04	0.17	0.02
Land	0.29	0.54	0.42
Sea-Ice	-0.21	-0.16	0.01
Snow	0.40	-0.19	-0.18



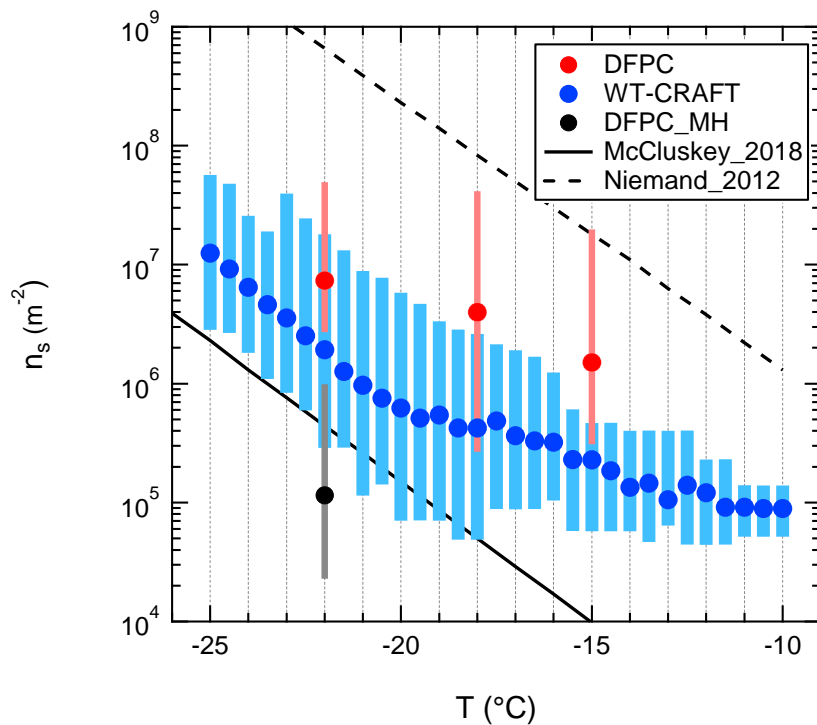
825 **Figure 1:** Atmospheric concentration of INP as a function of the activation temperature measured at GVB during 2018 by DFPC (PM₁₀) and WT-CRAFT. Dots indicate the median value, while bars span from minimum to maximum. DFPC dataset does not present samples with below detection limit concentrations. For WT-CRAFT, only data above the detection limits were used.



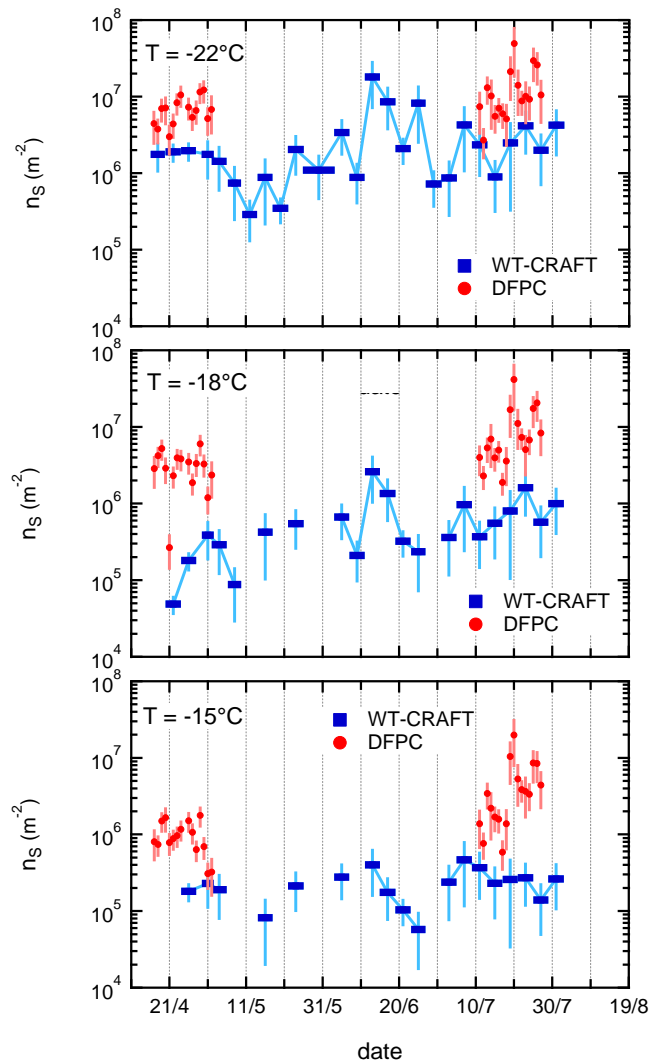
830 **Figure 2:** WT-CRAFT immersion freezing n INP spectra for the experiments exhibiting ice nucleation at $T > -15$ °C. Our spectra are superimposed on the Wilson et al. (2015) max-min ice nucleation spectra for Arctic marine microlayer samples (adapted from Fig. 4a of Irish et al., 2017) for comparison (red shaded area). Three previous parameterizations (D10: DeMott et al., 2010, C86: Cooper, 1986, and F62: Fletcher, 1962) are also superimposed for comparison.



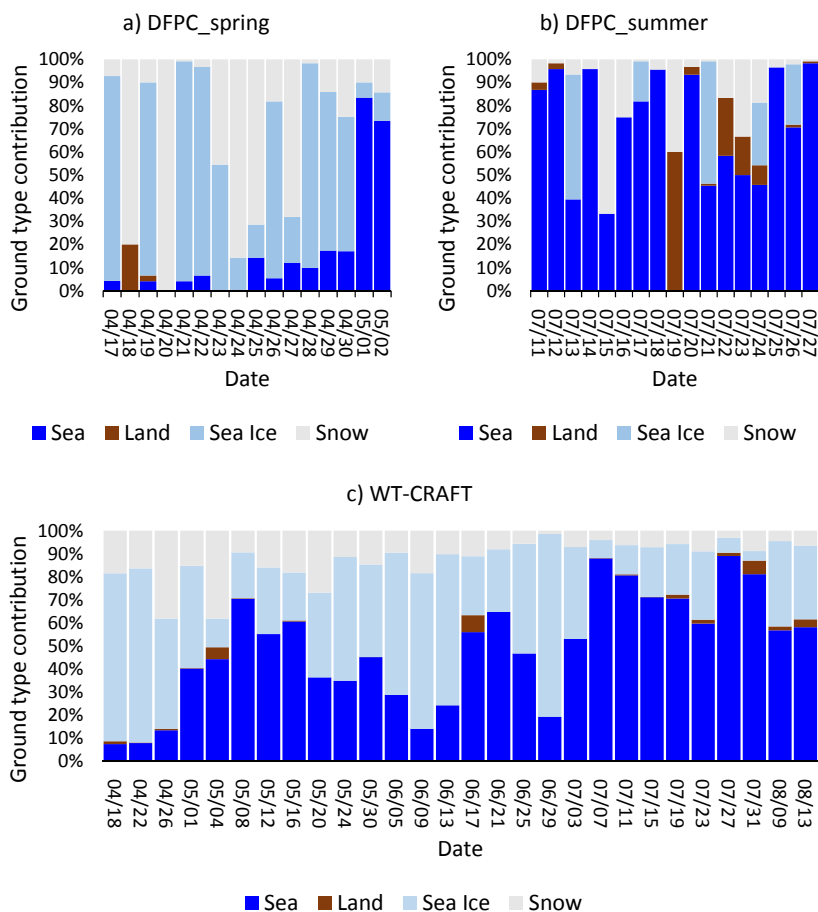
835 **Figure 3:** Time series of n_{INP} at GVB during 2018 measured by DFPC (PM_{10}) and WT-CRAFT. Horizontal bars indicate the time span of WT-CRAFT samples (ca. 4 days for the majority of samples). Vertical bars indicate the overall measurement uncertainty.



840 **Figure 4:** Ice nucleation site density as a function of temperature measured at GVB during 2018 by DFPC and WT-CRAFT. The parametrizations by Niemand et al. (2012) and McCluskey et al. (2018) are also reported, for comparison purposes, together with DFPC measurements performed in clean marine air masses at Mace Head. Dots indicate the median value, while bars span from minimum to maximum.

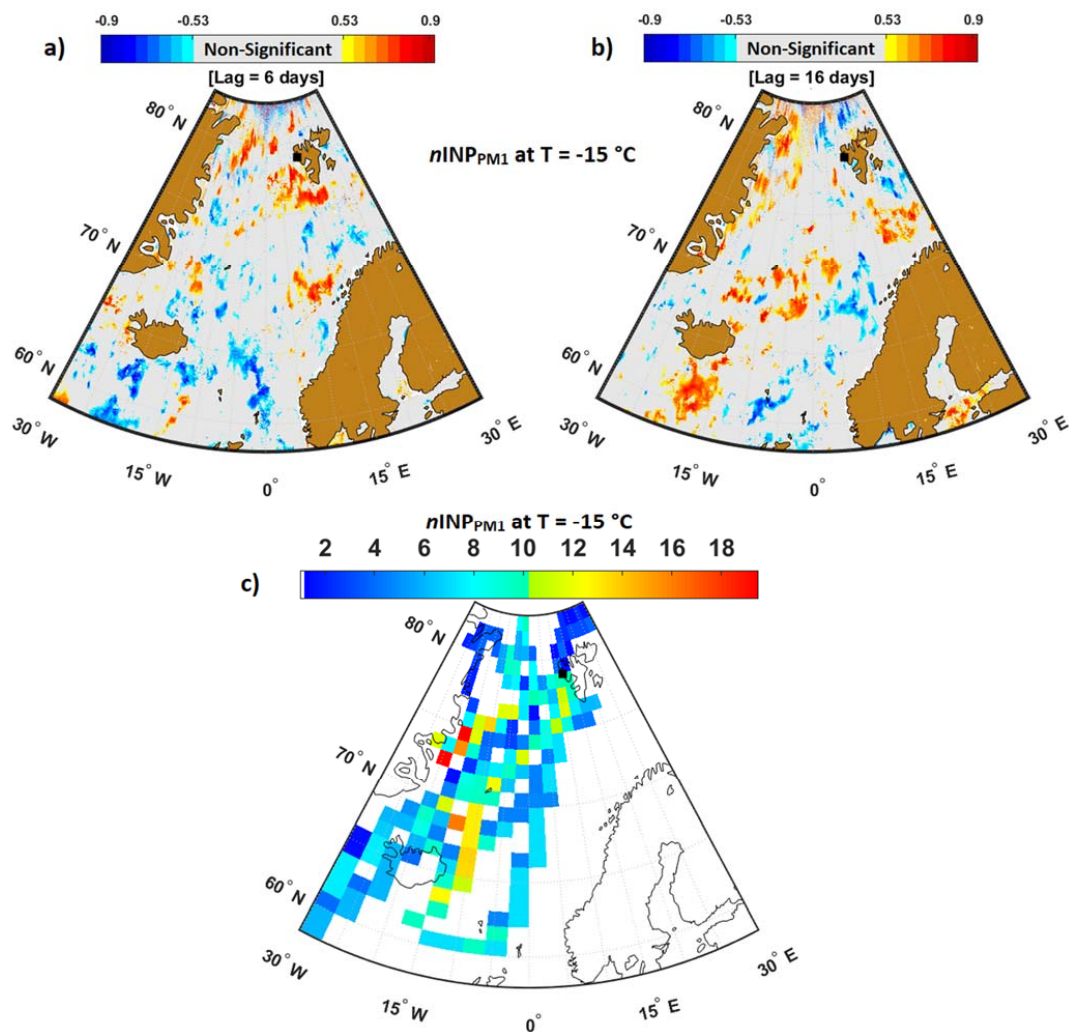


845 **Figure 5:** Time series of the ice nucleation site density at GVB during 2018 measured by DFPC (PM₁₀) and WT-CRAFT. Horizontal bars indicate the time span of WT-CRAFT samples (ca. 4 days for the majority of samples). Vertical bars indicate the overall measurement uncertainty.



850

Figure 6: Ground type influence on low-travelling (<500 m) air masses for DFPC in spring (a), DFPC in summer (b) and WT-CRAFT (c) measurements.



855 **Figure 7:** Correlation maps for $nINP_{PM1}$ at $T = -15^\circ\text{C}$ with (a) 6 and (b) 16 days time lag. Samples with clear land influence (3) were removed from the analysis. The color scale indicate the correlation coefficient. (c) CWT source maps for the same dataset. The color scale indicate the CWT value.